45 p.

NASA TECHNICAL NOTE

NASA TN D-1903

NASA TN D-1903

ARIEL I—EVOLUTION OF ITS STRUCTURE

by Carl L. Wagner, Jr.;
Goddard Space Flight Center,
Greenbelt, Maryland

NATIONAL AERONAUTICS AND SPACE ADMINISTRATION • WASHINGTON, D. C. • SEPTEMBER 1963

TECHNICAL NOTE D-1903

ARIEL I - EVOLUTION OF ITS STRUCTURE

By Carl L. Wagner, Jr.

Goddard Space Flight Center
Greenbelt, Maryland

NATIONAL AERONAUTICS AND SPACE ADMINISTRATION

ARIEL I - EVOLUTION OF ITS STRUCTURE

by
Carl L. Wagner, Jr.
Goddard Space Flight Center

SUMMARY

20605

The world's first international satellite, Ariel I, was launched April 26, 1962, after almost two years of cooperative effort between the United Kingdom and the United States. The structure of any spacecraft is a complicated system, the development of which involves design, development, and testing of mechanisms as well as structural components. The time scale from inception to launch of Ariel I required overlapped scheduling of its design, fabrication, and testing. The extensive development program described herein culminated in a structure that successfully survived a rigorous and unscheduled injection sequence to become a successful and useful orbiting spacecraft.

CONTENTS

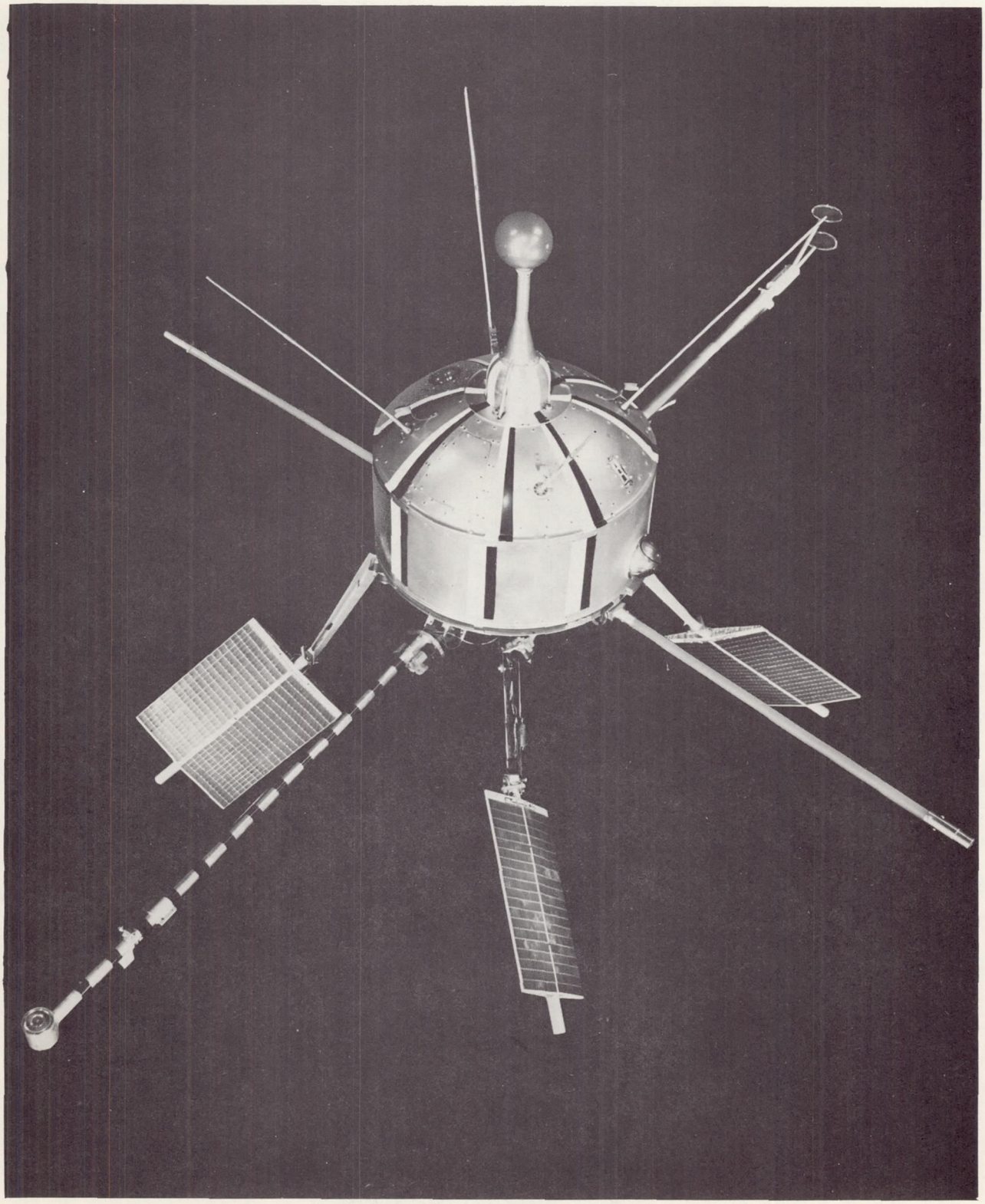

Ariel I in orbit attitude.

ARIEL I - EVOLUTION OF ITS STRUCTURE

by
Carl L. Wagner, Jr.
Goddard Space Flight Center

INTRODUCTION

Ariel I (1962 σ1) was the direct result of a United States proposal during the 1959 COSPAR meeting, in which the U. S. Government offered to launch experiments of mutual interest designed by foreign scientists. The United Kingdom accepted the offer, and a joint effort that culminated in the successful launching of "Ariel" (named by the U.K.) was undertaken. The Goddard Space Flight Center (GSFC) was responsible for—among other things—the design, fabrication, and testing of the spacecraft structure. Design of the structure began in May 1960.

STRUCTURE DESIGN PROGRAM

The structure design was originally governed by the limitations of the Scout vehicle and by the use of reliable "off-the-shelf" components. Of course, it was required to contain and support all experiments and electronic components.

The task of supplying a structure was accomplished in the following overlapping steps:

1. Definition of parameters
2. Design
3. Manufacture of antenna model
4. Manufacture of engineering test unit (ETU)
5. Testing ETU, and modification of design
6. Manufacture of pre-prototype and prototype
7. Final design tests and modifications
8. Manufacture of flight units 1 and 2
9. Final qualifications, and preparation for launch

The effort culminated in a structure that successfully withstood the rigors of powered launch; high speed erection of its antennas, solar paddles, and experiment booms; separation from the vehicle; and injection into a useful orbit about the earth. Figure 1 shows the basic development schedule used.

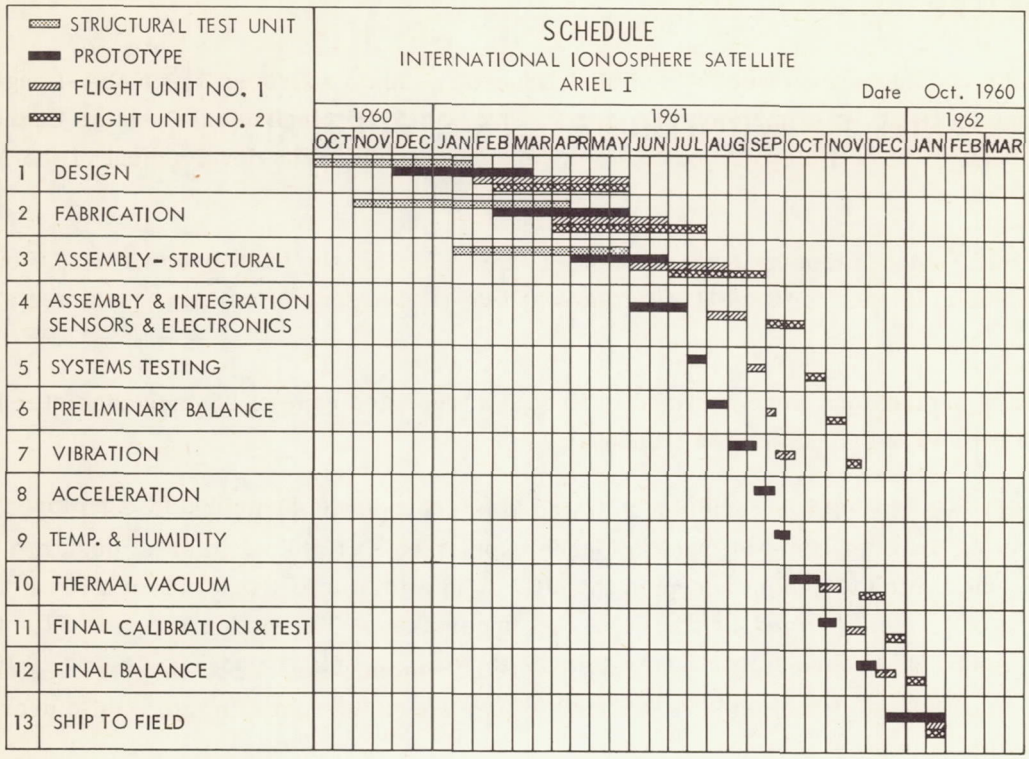

(a) Planned

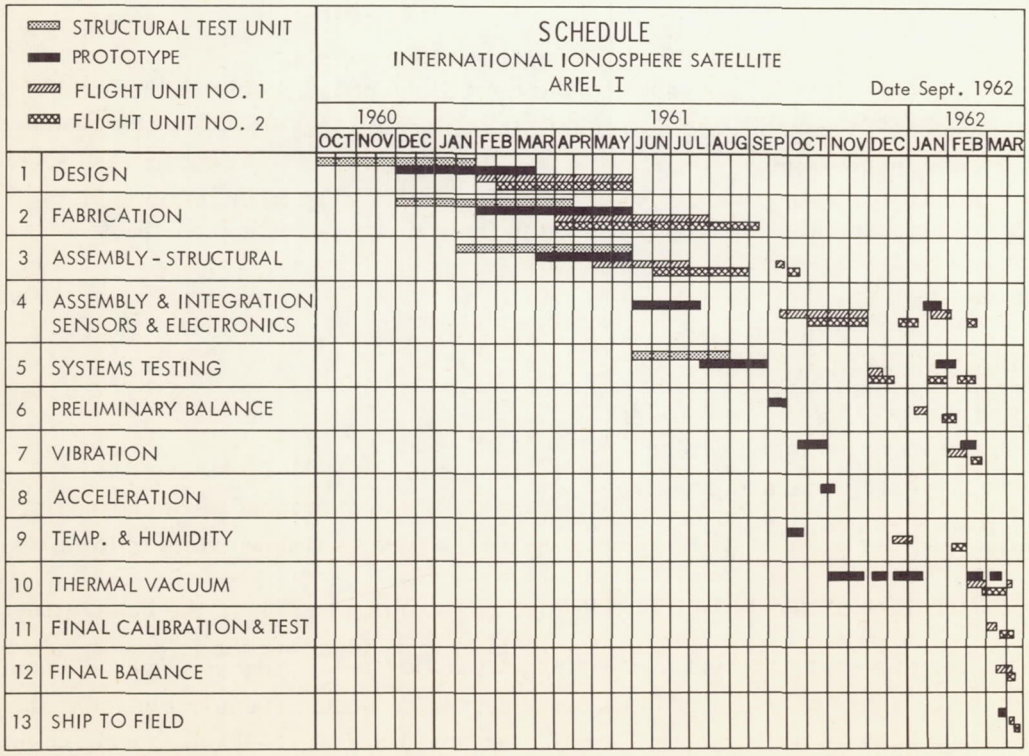

(b) Actual

Figure 1—Ariel I development schedule.

DESIGN PARAMETERS

Data for design considerations were assembled from three main sources: the NASA-Langley Scout Vehicle Manual, the U.K. experimenters, and the overall GSFC Mechanical Systems Branch experience and "bylaws." The following parameters were paramount in the development of the Ariel I structure:

1. The Scout 25.7-inch-diameter nose cone (heat shield) limited the basic payload to 23.0 inches in diameter by 2 feet in length, not including forward and aft protrusions of certain experiments and appendages.

2. The forward protrusions were confined to fit into a truncated cone of 23-inch-diameter base by 14 inches high by a 14.8-inch-diameter truncation.

3. The aft appendages had to be contained during launch in a space described by a hollow cylinder of 23 inches O.D. by 18 inches I.D. by 4 feet 8 inches in length.

4. The orbiting spacecraft would weigh no more than 135 pounds.

5. The structure was required to be manufactured of non-metals and/or non-magnetic materials so that effects of magnetic spin damping are reduced. The planned 36-rpm spin rate was to decrease after 1 year to a final spin of no less than 12 rpm.

6. Useful satellite lifetime was set at 1 year in orbit.

7. Off-the-shelf items were utilized in the design wherever possible.

8. The structure had to withstand, and was required to protect experiments and electronic components from, the rigors of vibration and accelerations during launch. In this case the ABL-X248-A5 solid-fuel rocket motor (last stage) governed. Outgassing products were to be minimized.

Test parameters are discussed later in this report.

SATELLITE STRUCTURE DESCRIPTION

General

As a result of the listed design considerations, fiber glass and aluminum were chosen for the structure materials. A description of the fully developed structure as it now exists follows.

The spacecraft structure should properly be divided into two main groups: the basic structure, and the appendages. The basic structure should then be further divided into the following subcomponents: *upper dome, mid-skin, shelf and base assembly,* and *lower dome.*

The appendages are as follows: *four solar paddles, two inertia booms, electron density experiment boom, electron temperature experiment boom,* and *telemetry antennas.*

Outer Structure

General

The material chosen for the skin of Ariel I is epoxy-bonded fiber glass. The domes are constructed from lengths of monofilament glass fibers loosely cross-woven into cloth laminations that are molded into a spherical shell of 13 1/2-inch radius by 5 5/8 inches high. Shell Epon 828 with a CL hardener is the bonding agent. The top dome is 1/16 inch thick, and the bottom dome—basically used only as a thermal shield—is 1/32 inch thick. The mid-skin is made from a cylinder of epon-bonded, monofilament, helical-wound fiber glass 1/16 inch thick by 23 inches in diameter by 10.7 inches long.

Upper Dome Assembly

Into the top of the upper dome skin is bonded and riveted an aluminum disk 8 1/2 inches in diameter by 0.2 inch thick. Machined integrally with, and centrally located on, the disk is a 7-inch-I.D. thin-walled cylinder extending internally 3.7 inches. This hat-shaped structure supports the cosmic ray - ion mass sphere experiments and the eight radial fiber glass ribs, which are also attached by rivets and bonding material to the dome skin, thus giving stiffness and strength to the dome. A machined aluminum ring is bonded and riveted to the base of the dome, allowing the assembly to be bolted to the top of the 23-inch-diameter mid-skin. Holes are cut in the proper places of the dome to allow attachment of experiments and antenna mounts.

Figure 2(a) shows the upper dome from the outside, and Figure 2(b) the inside of this component.

Mid-Skin

The mid-skin fiber glass is bonded and riveted to two end flanges, machined from AISI 6061-T6 aluminum, which are shaped to provide nonshifting attachment to the upper structure and the shelf-base assembly. In detail, shear lips prevent radial movement of the skin components, pins prevent rotational displacement, and machine screws tie these components together. Figure 2(a) shows the mid-skin and the Lyman-alpha detector adapter ring riveted to the cylinder.

Lower Dome

The fiber glass lower dome is segmented and fitted with aluminum doublers for installation of sensors and the segments themselves. Gold-plated aluminum machine screws hold these components in position. Figure 2(a) shows this component also. The skin components in this figure are not yet surfaced with the thermal coatings of copper, gold, lacquers, and paints.

Shelf and Base Assembly

General

The instrument shelf and base assembly (Figure 3) is made from AISI 7075-T-6 and AISI 6061-T6 aluminum plates, bars, and billets machined into shape and semipermanently affixed into the assembly condition. The separate parts are the following.

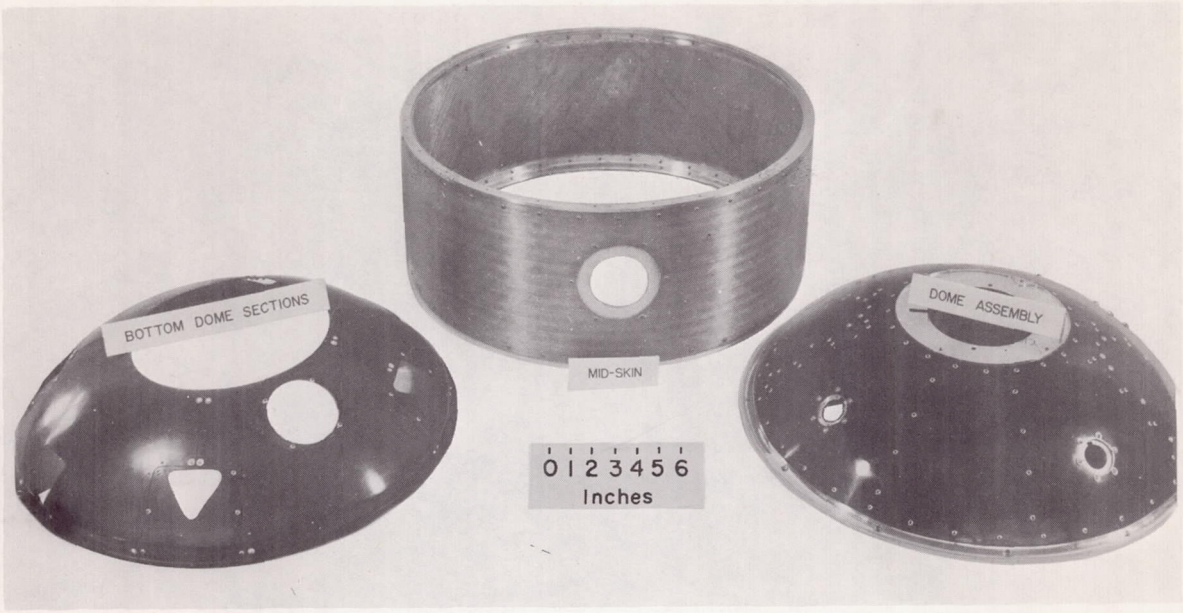

(a) Uncoated upper and lower domes and mid-skin

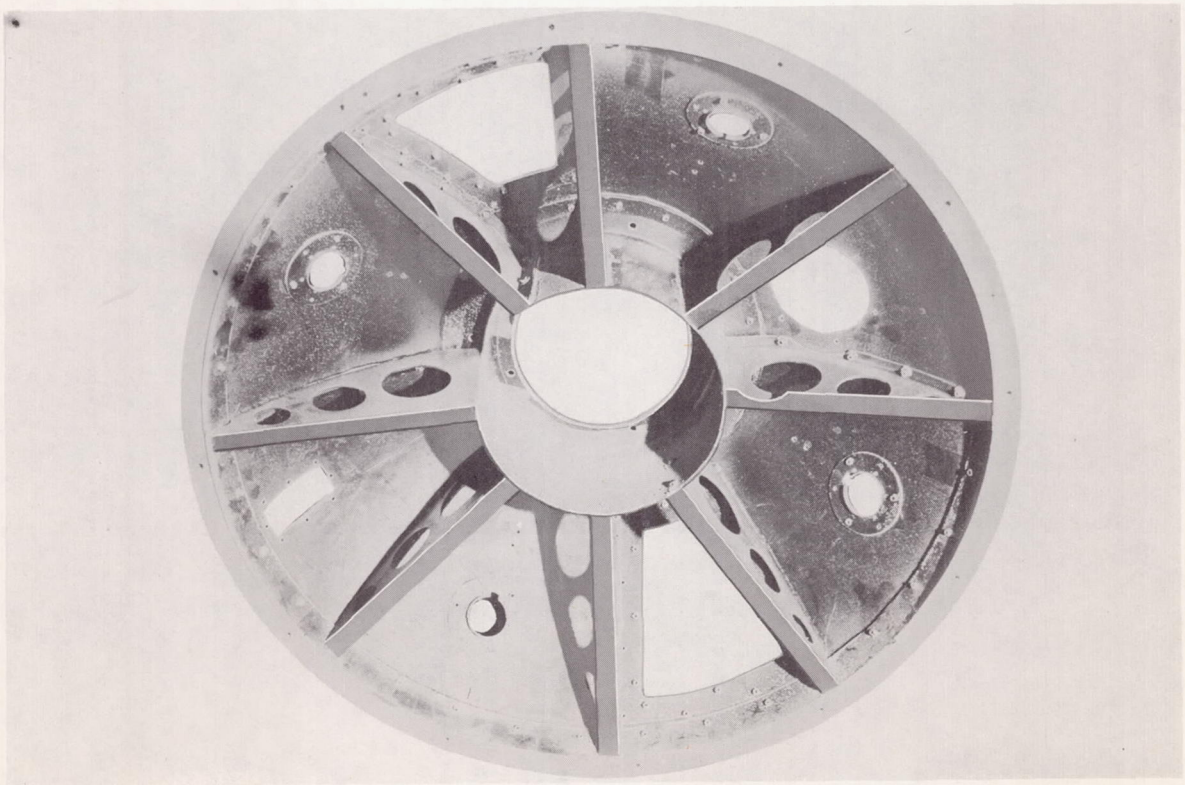

(b) Interior view of upper dome

Figure 2—Domes and mid-skin.

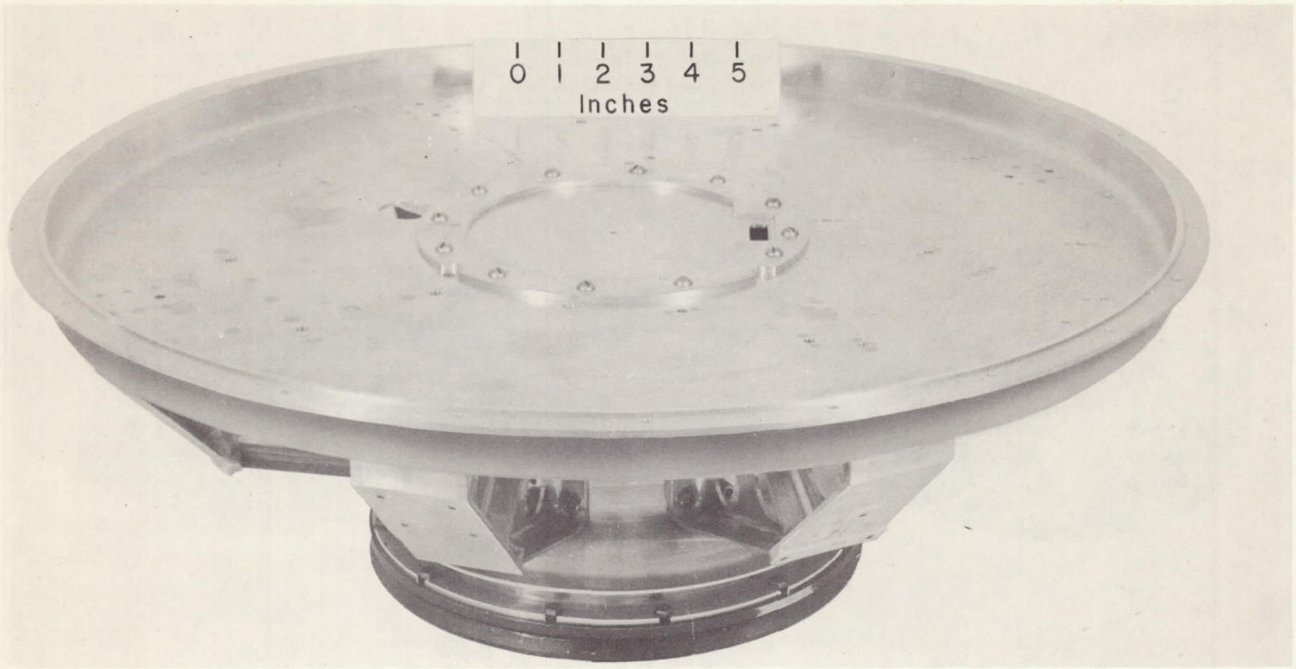

(a) Viewed from above

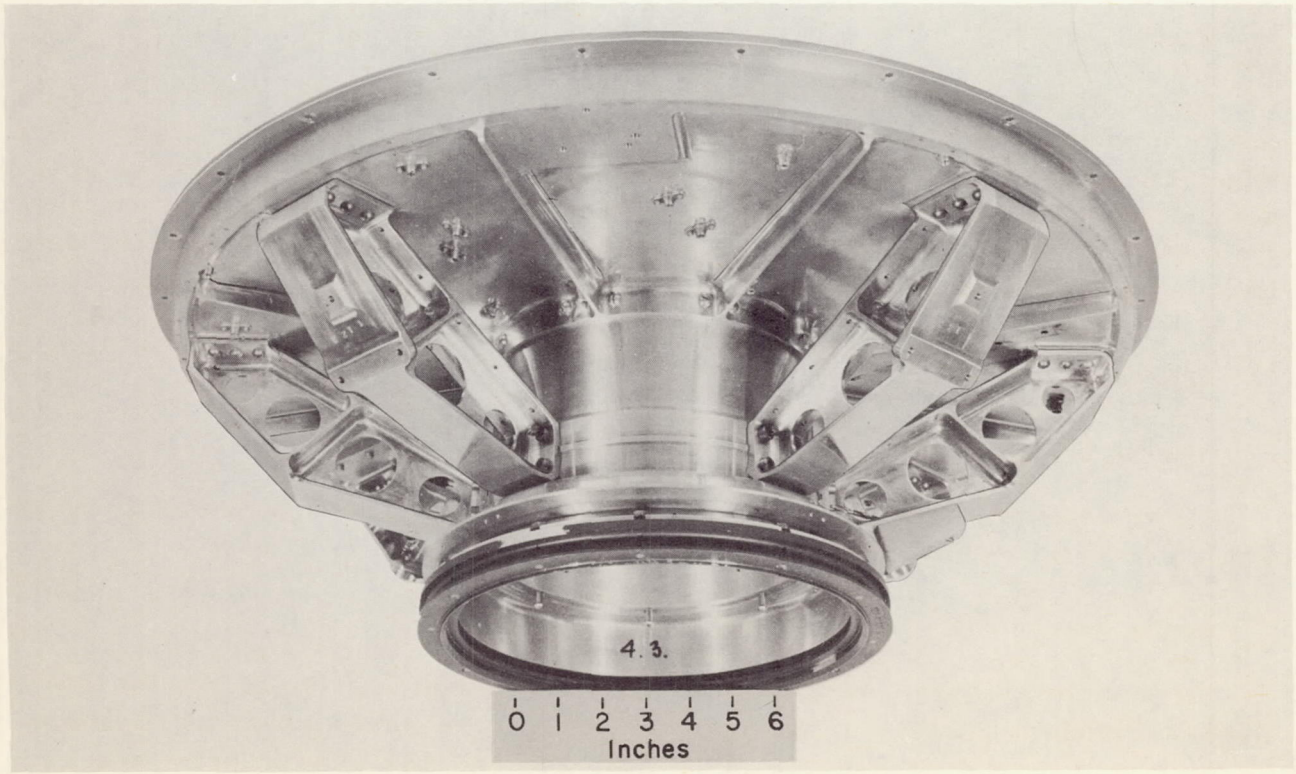

(b) Viewed from below

Figure 3—Electronic shelf and base assembly.

Shelf

The shelf is basically a 21-inch-diameter plate 0.08 inch thick with eight integrally machined stiffening ribs leading radially from a 7 1/2-inch-diameter integral ring to the outer periphery. This undercarriage of ribbing tapers from 0.7 inch at the cylinder to 0.3 inch at the 21-inch-diameter periphery [Figure 3(b)]. The top or forward face of the shelf at the 21-inch diameter is dished upwards for 1 inch and then again extends radially until the shelf reaches 23 inches in diameter. This step is so machined to supply room for the de-spin system and to provide a mating surface for the mid-skin. Figure 3(a) also shows the shear lip at the mid-skin interface.

Base

The base is a cylinder of 7 inches I.D. fitted into the 7 1/2-inch-diameter under-shelf ring, and then extends aft for 6 1/2 inches. The aft 2 inches is machined to an 8 1/2-inch inner diameter to provide proper view angles for the spin-axis-mounted aft-viewing electron temperature sensor. The forward 7-inch-diameter by 4 1/2-inch-long space is provided for containing the above sensor, the satellite's tape recorder, and the boom escapement mechanism. The outer diameter is machined to provide (1) a mounting surface for the separation adapter ring, (2) a mounting surface for the bottom dome segments, and (3) a key for six support struts. Figure 3(b) also shows the separation adapter ring.

Struts

The six struts are each machined from solid stock and take the shape of a modified "I" beam. Each strut serves to support the shelf and to supply the mount for a paddle arm or experiment boom hinge. The struts are keyed to the base and, after being fastened into position with machine screws, keyed to the shelf by shrink-fit shear pins. Space considerations prevented the use of a strut for the inertia booms, and therefore the shelf was thickened in the areas required for attaching these boom hinges. Figure 3(b) locates one of these pads in the upper center portion of the photo.

Appendages

General

The eight appendages should be considered in three separate groupings: paddle arms; inertia arms; and sensor, or experiment, booms.

Paddle Arms

The paddle arm and hinge design was suggested by that used on Explorer XII (1961 υ1); however, space considerations dictated by the Scout heat shield and paddle-location restrictions required by the experiments complicated the design considerably. The arms themselves are long slender channels machined from AISI 7075-T6 aluminum. One pair of arms leads directly from the hinges to the paddle interface, but space and positional requirements for the other pair of solar paddles required

a secondary folding hinge at the outboard end of each arm. From this secondary hinge extends the paddle interface of these two arms. Figure 4 shows these arms and the spars to which the paddles themselves are assembled.

Inertia Booms

The inertia booms are used to provide the proper moment of inertia ratio; that is, $(I_s/I_p) > 1$, where I_s is the moment of inertia about the vertical or spin axis and I_p is about either of the other two principal axes perpendicular to the spin axis. When this ratio is satisfied, the satellite will continue to spin about the original spin axis rather than begin to tumble about it. The moments of inertia are listed in Appendix A. These inertia booms are made of thick-wall tubes of epon-bonded fiber glass cloth rolled into cylindrical shape. Each boom is attached to the shelf by a detent-locking, spring-loaded hinge; and at the outboard end of its 30 inches is a 0.7-pound steel weight, 4 inches long (Figure 4). Both the inertia booms and the paddles are designed to erect at 52.4 rpm, reducing satellite spin to 36.6 rpm.

Experiment Booms

The sensor, or experiment, booms are made by the experimenters, but the method of attachment and erection is part of the structure design responsibility. The hinge halves are machined from solid stock aluminum and use a double detent lock. A torsion spring imparts positive force to assure opening in the event of no payload spin-up. (This consideration is true in all appendage extension.) Figure 5 shows the experiment boom hinge.

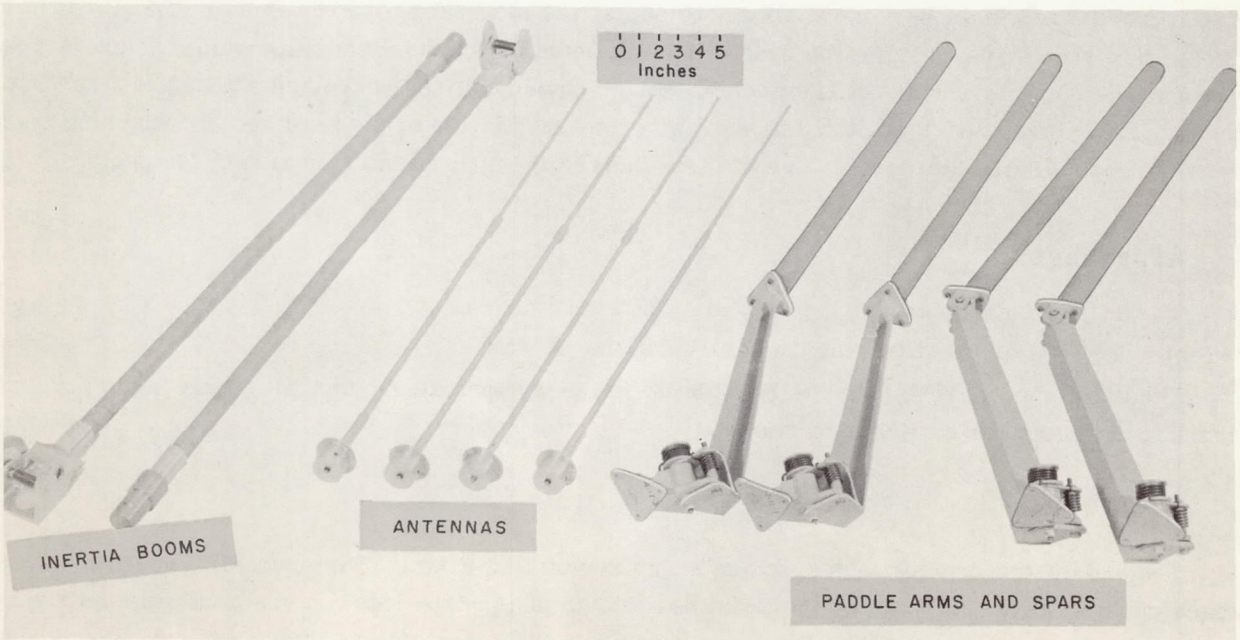

Figure 4—Satellite appendages.

Escapement

Normal rotational speed of experiment boom erection is 76.5 rpm, which would produce large shocks to the experiment sensors if these booms were allowed to open without restraint. As a result, an escapement device reduces these forces by controlling erection speed. Figure 6 shows the escapement mounted on the base closure plate.

The clock escapement principle is employed in the design of this timing, or restraining, mechanism. Since the primary interest in the application is to reduce shock, and not in the accuracy of timing erection, the less sophisticated mechanism, called a *run-away-escapement,* is used. It consists of a gear train coupled to an escape wheel, and a pallet fitted over the escape wheel to control its rotation rate. The two booms are required to be controlled simultaneously; thus a double pulley mounted on a common shaft is coupled to the free end of the gear train. A doubled nylon cord with one end attached to the boom and the other end to the pulley serves as the control linkage. The escapement's rotation rate is a function of the satellite actuation torque and the moment of inertia of the pallet. This moment of inertia is adjusted to allow the booms to erect in 2 to 3 seconds. This escapement successfully controlled boom erection when the satellite spin rate was between 60 and 90 rpm (Reference 1). The simultaneous boom erection prevents any unbalance that would contribute to unwanted coning of the payload. (The other appendages open quickly enough to avoid this problem.) The planned sequence of appendage erection is given in the following list; each group of appendages was designed to survive the forces of erection of the preceding step.

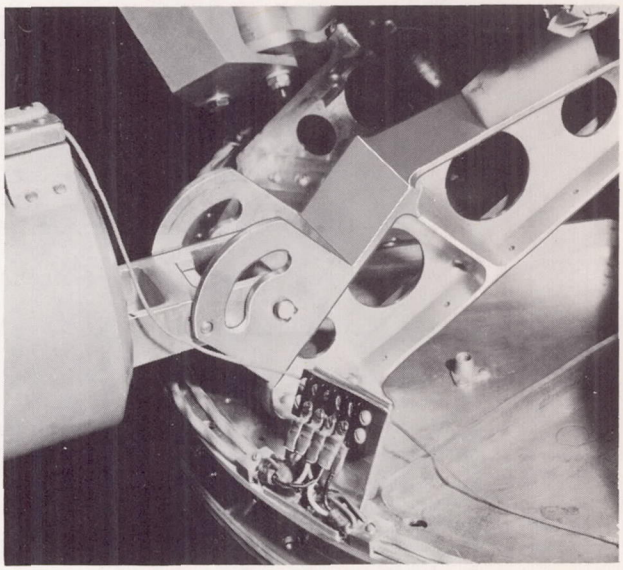

Figure 5—Experiment boom hinges.

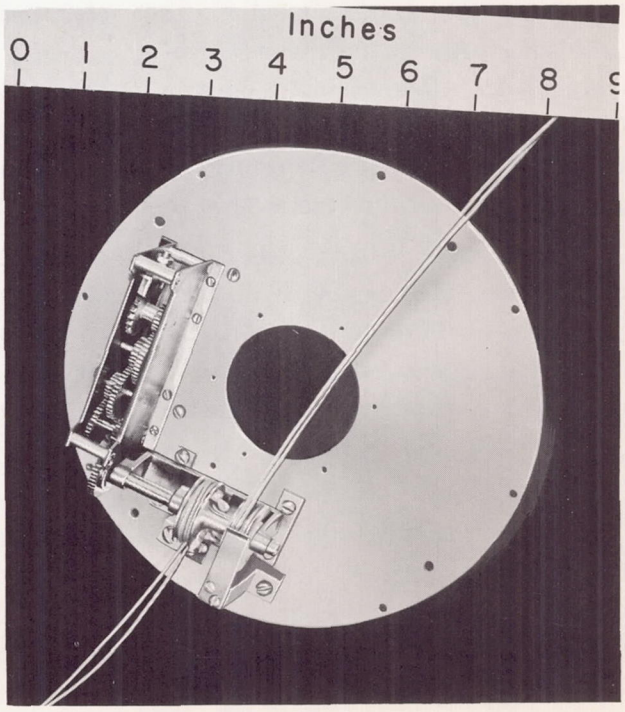

Figure 6—Escapement device mounted on base closure plate assembly.

Proposed Spacecraft Injection Sequence*

The sequence of events from nose cone ejection to satellite separation is as follows:

1. Nose cone ejection and erection of spacecraft antenna

2. Second-stage burnout

3. Second- and third-stage coast and yaw until peak of ascent path is reached and vehicle is aligned with its programmed attitude

4. Third-stage spin up to approximately 160 rpm (T-0)

5. Third-stage ignition, second-stage separation, and retrorockets fired (T+15 sec)

6. Burnout of third stage (T+42)

7. Coast to allow outgassing (thrust) of the third stage to cease (15 min duration)

8. De-spin of the third-stage - payload combination to 76.5 rpm, by releasing "yo-yo" de-spin device (T+900)

9. Release and erection of experiment booms and de-spinning to 52.4 rpm (T+960)

10. Release and erection of the inertia booms and solar paddles, de-spinning to 36.6 rpm

11. Separation of the payload from the third stage at a differential velocity of 7 ft/sec

De-Spin Device

The de-spin system is built in a self-contained ring fitting in the space provided at the periphery of the shelf. It is of the "stretch yo-yo" design, which will de-spin a system having a ±20 percent nominal spin rate error to ±2 percent of the required final value. The basic components are a pair of equal weights attached to a matched pair of long tension springs wound one-half turn about the payload. The weights are released by guillotines, and the weight-spring combinations unhook themselves when in a radial attitude from the spacecraft; by this system the payload is de-spun from 160 to 76.5 rpm.

The original de-spin design utilized a pair of constant length wires to which were attached the end masses. This system is accurate enough in reducing spin of a known value; however, should this original spin be 15 percent in error, the de-spun value would be equally in error. (References 2 and 3 fully discuss the stretch yo-yo design.) The stretch yo-yo concept was utilized, and the de-spin system was redesigned to assure more accurate de-spin of the satellite.

Antennas

The four turnstile-type antennas are of the double-fold design, required by the space limitations of the Scout heat shield. These antennas are located 90 degrees apart on the top dome, and in their erection position make an angle of 40 degrees with the spin axis. Upon ejection of the heat shield, the antennas unfold to lengths of 21 3/4 inches. The thin-wall aluminum sections contain tension springs that open the antennas and lock mating coned interfaces to create a rigid antenna. Figure 7 shows a set of these antennas with one primary hinge folded; Figure 8 shows the antennas in place on the flight unit.

*Final rate of spin at the end of 1 year should not be less than 12 rpm.

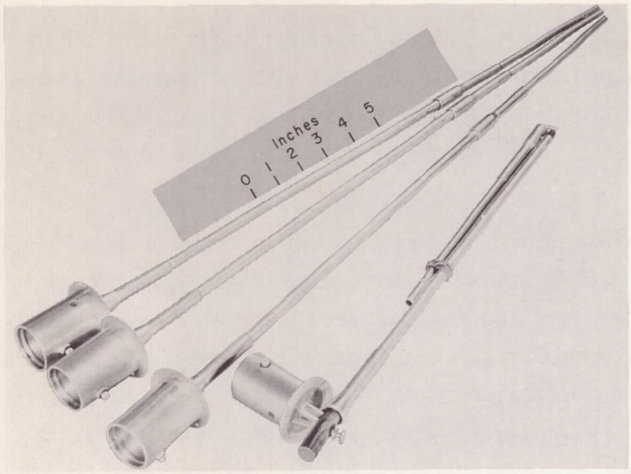

Figure 7—Flight antennas.

Battery Containers

The spacecraft power storage and supply system is separated into two equal packages of 10 sealed Gulton nickel-cadmium battery cells each. Either package is sufficient to operate the spacecraft. The 10 batteries are divided into two stacks of 5 each. Tests have shown that each stack of batteries, when operated under adverse conditions, would expand—in fact, could even burst. This expansion is in the direction that would cause unrestricted stacks to grow taller. The battery containers were designed to resist this force and thus prevent contamination of the spacecraft due to a possible battery rupture. These structurally rigid packages are firmly attached to the shelf above each inertia boom hinge pad, thus giving added strength and stiffness to the shelf. Figure 9 depicts the battery container.

Miscellany

The above paragraphs have described the main components of Ariel I; but no system is complete without brackets, and Ariel I is no exception. The electrical harness is built around, and supported by, a center support tube and

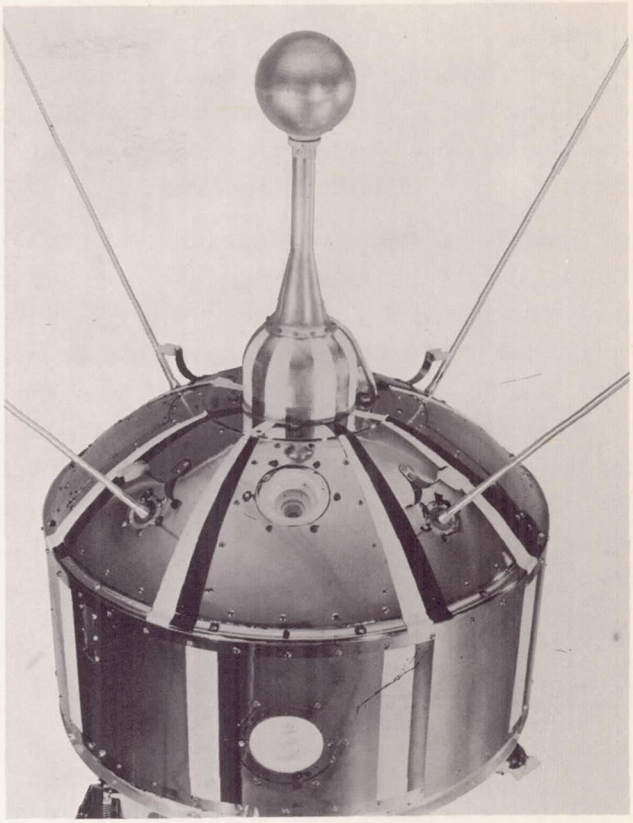

Figure 8—Antennas mounted on the flight unit.

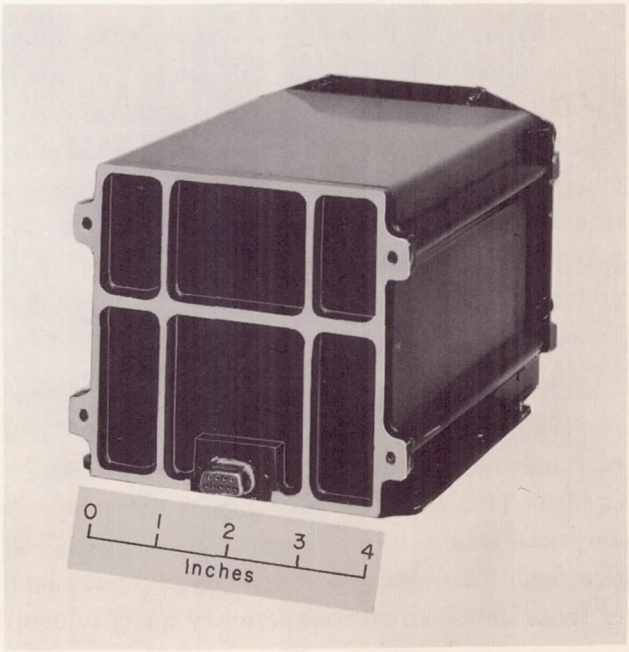

Figure 9—Battery container.

bridge assembly. The turn-on plug is housed in a specially designed receptable and plug assembly. Pyrotechnic device connectors are protected from stray RF by special covers. Small components that do not mount on the shelf require brackets and adapters designed to meet each situation. The above bracketry, supports, and fasteners plus the main structure mechanisms and components account for 50.6 pounds of the orbiting spacecraft. A list of the weights of the components discussed in this report is included in Appendix A.

During the assembly, integration, testing, and pre-launch field preparation of Ariel I special handling gear was required: e.g., the assembly dolly, lifting adapter, protective covers for experiment sensor, and shipping containers. Specialized alignment and test fixtures were also necessary, such as the paddle arm alignment fixture, moments of inertia measuring gear, a nonmagnetic support stand for antenna pattern determination and experiment calibration. Two variable-speed multiposition spin tables were required: one for preliminary quarter-scale solar aspect determinations, and the other for two purposes: (1) When equipped with a freewheeling clutch, it was used for appendage release testing; and (2) when equipped with elevating mechanisms, it was utilized in flight solar-paddle power output calibrations. These handling gear and alignment fixtures, although not part of the structure, were necessary to the program and were designed by the GSFC structures group to fill their special needs.

TESTING OF THE STRUCTURE

General

Tests conducted on the Ariel I structure can be divided into two main categories: design tests, and qualification tests. The design tests were conducted by, and/or for, the GSFC mechanical design team; the qualification tests were conducted for the most part by, and with, the GSFC Test and Evaluation Division. One test series, appendage erection and de-spin tests conducted at Langley Research Center vacuum facilities, was considered a combined design and qualification test series. Certain tests were involved in nature and major in scope; others were short, informal assurances. Informal assurance tests have been compiled into a single document.* Only those tests considered to be major in respect to structure development are reported herein. Even so, the number of tests grows large; therefore, discussion will be kept as short as possible. The tests will be grouped according to the structure unit on which they were conducted: engineering test unit, pre-prototype, prototype, and flight models 1 and 2.

Non-Structure Models

Early in the design phase of any satellite structure, an antenna model—a mockup generally describing the outline shape of the proposed structure—should be fabricated and used to test compatibility with the T/M antenna systems. This was accomplished with Ariel I, and the antenna pattern and other related tests established that the proposed structure would provide a sound ground plane, that antenna location in the satellite was satisfactory, and that no major T/M-RF problems were anticipated. Figure 10 shows the assembled antenna model.

*LeDoux, F., "Compilation, Design Tests Ariel Satellite (S-51)," GSFC X-634-62-157.

A second important test series, which did not involve actual structural components, required the use of a quarter-scale replica of the proposed structure (see Figure 11). This scaled model was fitted with solar cells, placed in a nonreflective environment, and subjected to collimated light. The model was rotated at 35 rpm, and its attitude to the simulated sun was varied to agree with the aspect angles expected for Ariel I in orbit. Voltage and current measurements were made, and were compared with those produced by a standard cell positioned perpendicular to the "sunlight." This test established that the solar paddle size, shape, and positions were satisfactory. Close agreement with theoretical predictions was established.

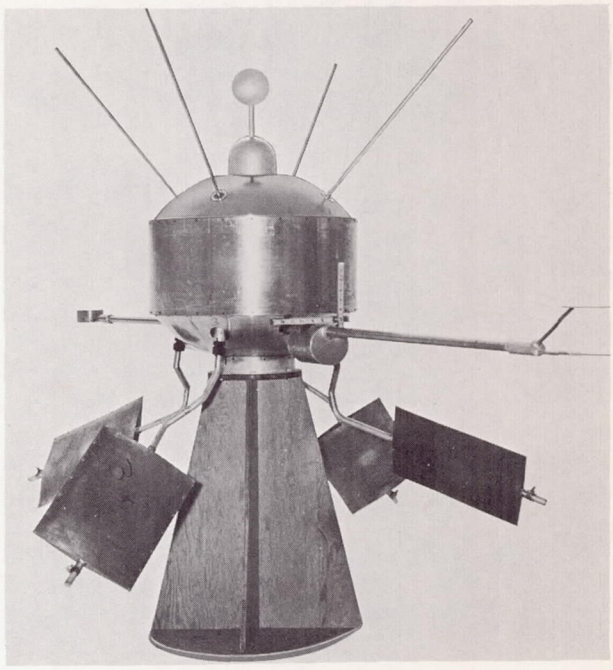

Figure 10—First full-scale antenna model.

Engineering Test Unit and Pre-Prototype Structures Tests

Vibration Testing

The structure was fitted with dummy electronic components and was vibrated on a fixture that simulated vehicle mounting as best known at that time. A 1 to 2 g sine sweep was conducted to spot structural resonances and possible areas of high transmissibility. Sine wave random noise and 600-cycle thrust vibration were programmed at flight and prototype levels (see Appendix B). As a result of this, test program weaknesses in the method of fastening the shelf, struts, and base into an assembly were discovered. A set of lifting rods designed to help tie the shelf assembly to the upper dome was found to produce unfavorable transmissibility levels to the upper dome components. The structure design was modified to omit the lifting tie rods, and the base-strut-shelf assembly was keyed with shear pins and interfaces, thus allowing the fasteners to be stressed in tension only. The ETU was then re-vibrated through the complete prototype schedule. No failures resulted, and the transmissibility levels to the upper dome components were lowered to a more satisfactory level. Further details may be found in Reference 4. Figure 12 shows the ETU

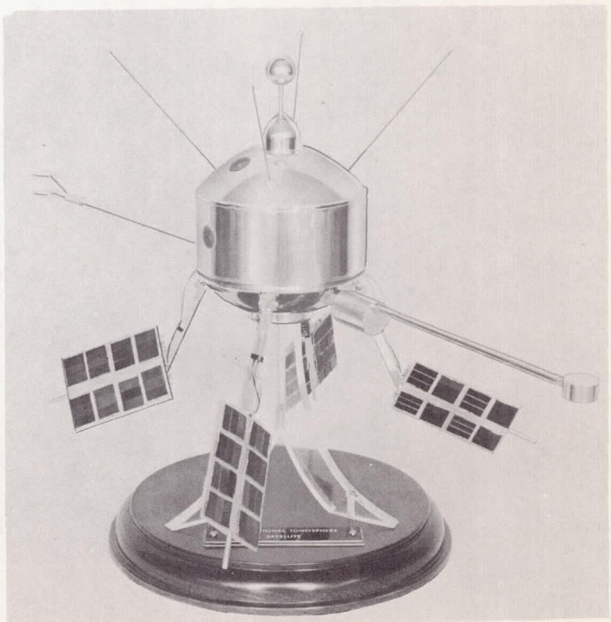

Figure 11—Quarter-scale model of Ariel I.

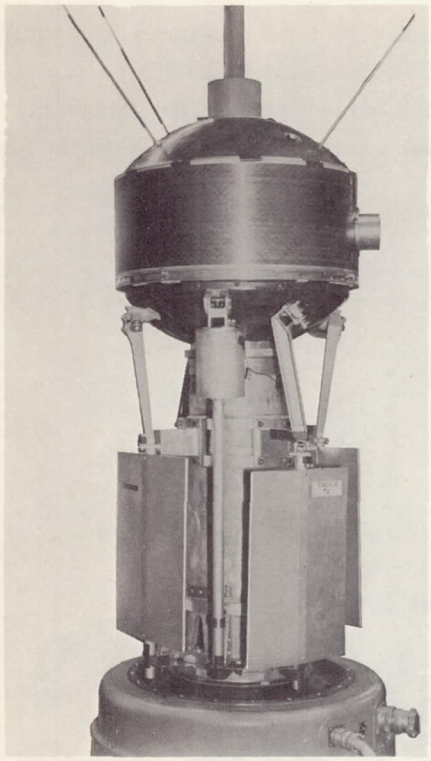

(a) "Low frequency" thrust vibration

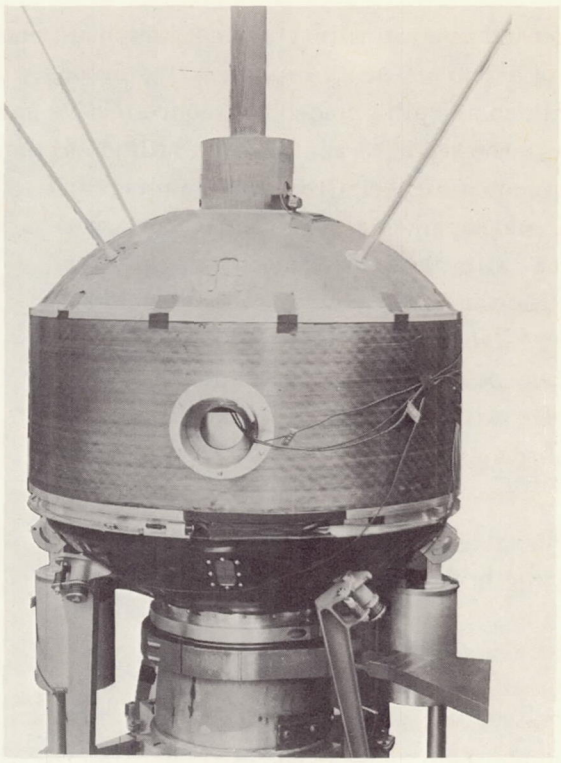

(b) "Low frequency" lateral vibration

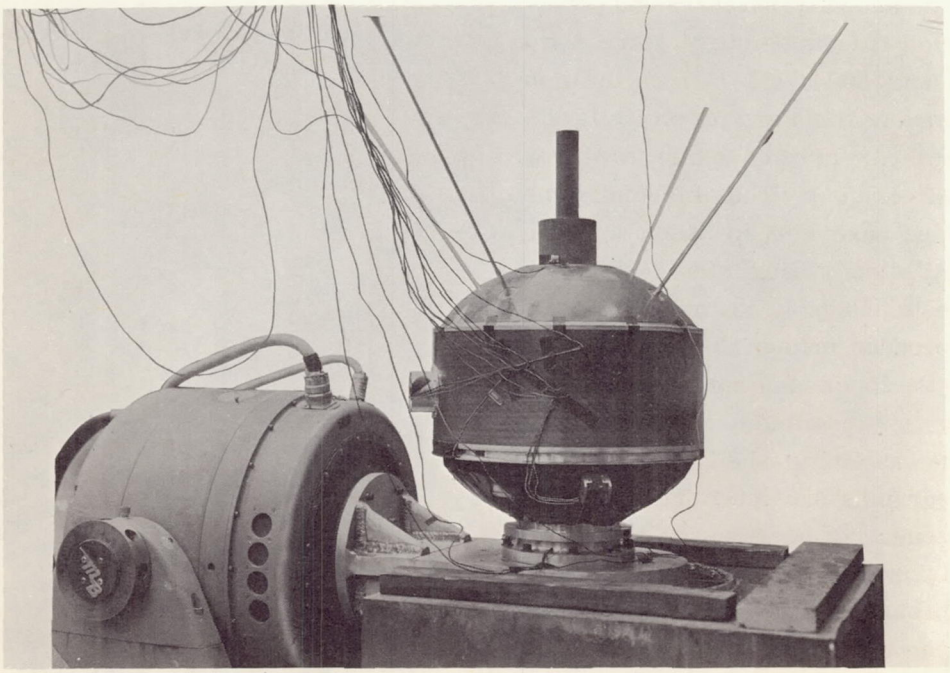

(c) "High frequency" lateral vibration

Figure 12—Engineering test unit.

mounted for low frequency thrust, low frequency lateral, and high frequency lateral tests [Figures 12(a), (b), and (c), respectively].

Acceleration Testing

The same structure was then subjected to steady-state accelerations simulating the flight environment produced by the X-248 rocket motor and to 1 1/2 times this environment (prototype level) in the thrust level. Prototype level accelerations were also applied to the structure in each of four transverse directions. The 20-foot-radius centrifuge located at the Chesapeake Bay Annex of the Naval Research Laboratory was utilized for the test series (see Figure 13). No failure was produced by these tests or by the inherent transportation vibrations resulting from trucking the payload to and from the test site. Table 1 lists the acceleration test levels of the series.

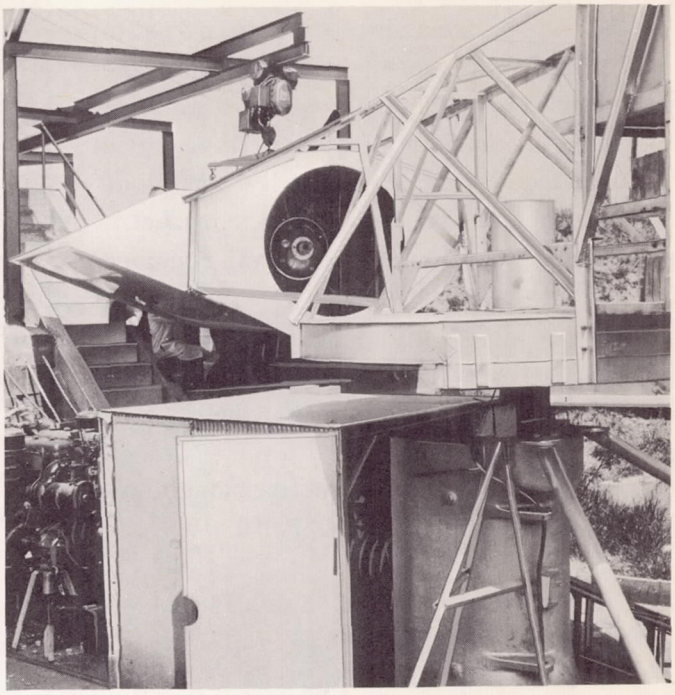

Figure 13—Engineering test unit at CBA centrifuge.

Moment of Inertia Study

The ETU structure—still with its full set of dummy components—was used for a moment of inertia study. Close agreement with calculated results was obtained, and important handling procedures and test methods were determined. The measured moment of inertia ratio of the proposed orbit condition of the satellite was $I_s/I_p = 1.01$; this was believed to be slightly marginal. It had been planned to increase the ratio by adding up to 10 pounds of ballast near the satellite's periphery, bringing the payload weight up to its allowable limit. This procedure was not used, however, because of a change in spacecraft weight requirements which is discussed later. In Figure 14 the payload is being measured for its moment of inertia about the spin axis.

Table 1

Steady-State Acceleration Test Specifications.

Test	Direction	Level* (g)	Remarks
1	Thrust	3.5	Used only during ETU study
2	Thrust	7.0	
3	Thrust	10.5	
†4	Thrust	14.0	Paddle weight and sensor boom simulators adjusted to impose correct test levels to respective hinges
‡5	Thrust	21.0	
**6	Lateral	3.0	Four directions, 90 degrees apart

*Duration of all tests, 1 min.
†Flight level acceleration.
‡Prototype level acceleration.
**Ground-handling simulation only.

RF and Thermal Coating

The application of the RF and thermal coating to the external surface of the skin proved to be one of the more severe environments the structure had to withstand. Several ambient temperature methods of producing the required thermal and electrical conductivity conditions were tried but could not be reliably reproduced. The following schedule of events was required to produce repeatable values:

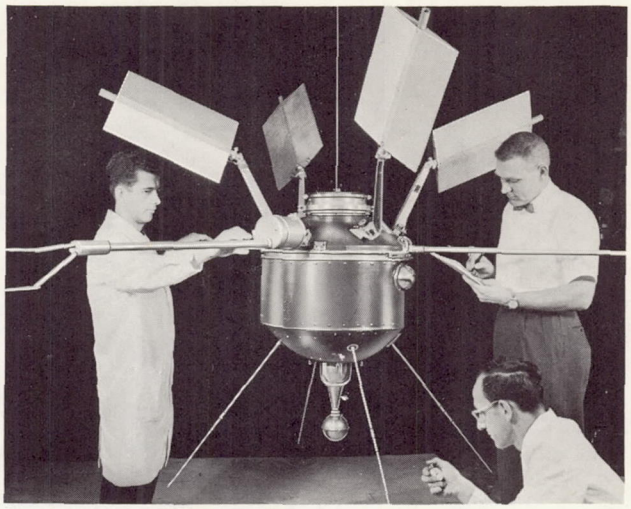

Figure 14—Ariel I being measured for moment of inertia about spin axis.

1. Bake the fiber glass to remove outgassing products - 300°F, 1 hour
2. Coat surface with conductive paint, thermal setting - 275°-300°F, 16 hours
3. Electro-deposit 0.001 to 0.0015 inch of copper, and buff to mirror finish
4. Coat surface with lacquer
5. Vacuum-deposit gold to 0.00004-inch thickness - 350°F for several minutes during the application, and buff to high polish

The combination of high temperature effects caused an unequal expansion of the fiber glass and the aluminum rings, as well as deterioration of the adhesive used to bond these components to each other. (Shell Epon 901 with a B-1 hardener was used for this purpose, since it did not require an oven for curing.) As a result, separation of the components occurred, thus destroying the structural integrity of the spacecraft. Two solutions were evident: (1) Change bonding agent and/or modify interface design, or (2) rivet the structural components into the skin assemblies. Method (1) required the use of a curing oven, "training" of the manufacturer, and was subject to failure. Method (2) required care and skill in assembly; however, this was within the capabilities of the manufacturer, and was the method chosen. "Pop" blind rivets were utilized, and subsequent thermal coating applications were successful; no detrimental effects to the structure resulted. (The frontispiece figure shows the satellite with its final thermal coating.)

Escapement Device

The testing and development of the escapement device, which limits the erection speed of the experiment booms, is the subject of a separate NASA report (Reference 5). The ETU and the preprototype structures were utilized for the numerous tests necessary in developing the escapement system.

De-Spin System

The design and preliminary testing of the proposed de-spin system, which utilized an end mass on each of two fixed lengths of cable, causing de-spin on release, were carried out by AeroLab of Pasadena, California. Function tests at AeroLab were performed under ambient conditions and used an inertia mockup for the payload. This mass was spun up to 180 rpm by air jets. Air supply was cut off just prior to actuation of the cable cutters. These function tests verified the design and proved that proper de-spin was obtained by the proposed system.

Weight Reduction Program

In July 1961, GSFC was advised that the Scout vehicle could not guarantee placement of the specified 135-pound spacecraft into its required orbit. A crash weight reduction program was immediately put into effect. The greatest single weight reduction was made by removing the 10-pound "passive" inertia mass and installing an "active" inertia mass system. This was composed of two small masses attached to fiber glass booms that were programmed to erect with the solar paddles. A net savings in weight of 6.1 pounds and a moment of inertia ratio gain to 1.07 I_s/I_p (from 1.01) resulted. The addition, however, required relocation of the lower x-ray sensor, aspect experiment, and shelf-mounted components, including separation of batteries from one container into two smaller ones located 180 degrees apart. The major areas of concern due to increased stresses were the shelf to which the inertia boom hinges were attached and, of course, the untried inertia boom hinges themselves. These hinges are similar in design to the experiment boom hinges. Figure 4 shows the inertia boom and its hinge.

Pre-Systems Test

A pre-systems test of appendage erection was then conducted prior to the all-systems test, which would be under vacuum conditions. This pre-systems test was conducted at the GSFC antenna range so that any malfunction would not damage the surrounding equipment, etc. To overcome the effects of gravity, the payload (pre-prototype) was spun at a higher rate than would be the injection rpm. Although a separate report (Reference 5) fully describes this test, a summary of the results is supplied herein. The problems areas uncovered are the following:

1. One secondary paddle hinge failed. Corrective action included a stronger, more positive, detent (or lock) action and redesign of hinge rotation limit stops, to change stressing action from shear over a small area to compression over a large (by comparison) area. Stress levels were thus reduced by a factor of 15 or more. (See Figure 15.)

2. Locking detents for all the booms were redesigned to allow faster action, and were made of stainless steel rather than aluminum. Reasons for the change: yielding and fracture of the original pins, and evidence that latching action did not take place on at least one detent—allowing the boom to fracture second detent and not remain in locked position. A "field fix" was instigated for use in the all-systems tests at Langley Research Center (LRC) vacuum facilities.

3. Paddle-to-spar fasteners showed some yielding; therefore, high-strength steel screws of no. 8 size rather than aluminum no. 6 were incorporated.

4. Timing of the sensor boom escapement was reinvestigated, resulting in a lighter weight on the escape pallet. This reduced pallet inertia produced a smaller restraining force on the booms, and allowed quicker action and more positive locking. (During low speed boom erection tests, the booms did not fully open; however, gravity is certainly a factor not completely eliminated by over-spinning an escapement restrained erection.)

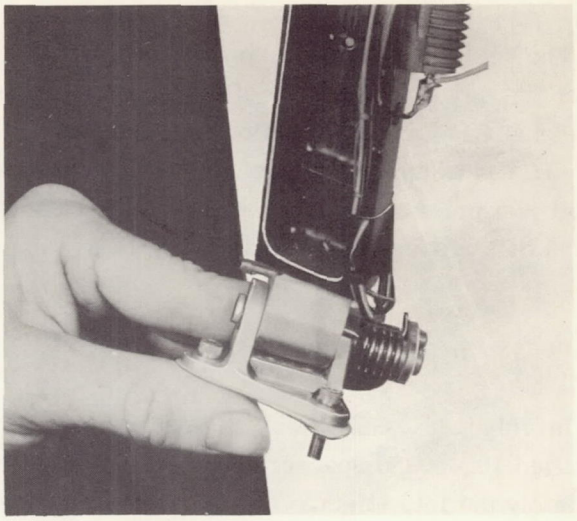

Figure 15—Final design of secondary paddle hinge.

All-Systems Sequence Test

An all-system structural function test was conducted at the LRC vacuum facilities in the 60-foot-diameter tank. The following functions were scheduled:

1. Spin-up with PET rockets: 2 trials with glass slides located at critical components to measure contamination deposits. A calibrated Lyman-alpha detector was also mounted in the lower dome for the contamination study.

2. Programmed de-spin of yo-yo, erection of experiment booms, and erection of inertia booms with solar paddles: 3 trials - nominal and ±10 percent of nominal speeds.

3. Separation of opened payload spinning at nominal and 10 percent under nominal rpm to determine tip-off and proper function.

Several weeks were involved in preparing the facilities; planned spin tables were burdened with excessive friction, and proposed slip rings and rpm counters were not at first compatible with proper test monitoring. A summary of the tests at LRC and their results are as follows:

1. Spin-up tests:
   (a) The structure is unaffected by spin-up.
   (b) The glass slides were not contaminated by four PET rockets.
   (c) The Lyman-alpha detectors showed less than 1 percent change as a result of each of two trials.

2. Yo-yo de-spin performed exactly as per calculation at nominal and ±10 percent of spin rate.

3. Booms and paddles, when erected, caused the spin rate to decrease as calculated, and will survive stresses of at least 10 percent excess spin rate.

4. A far more severe test was created when miswiring inadvertently caused all components to erect simultaneously from one signal, virtually de-spinning the spacecraft from 180 rpm to near 0 in one revolution. The following failures were evidenced:

(a) The three fasteners holding each of the inertia boom hinges to the shelf fractured in tension.

(b) The nylon cords linking the experiment booms to the detents failed in tension.

(c) The experiment boom hinge-to-strut fasteners (4 each) yielded, but did not fracture.

(d) The solar paddle hinge-to-strut fasteners fractured (paddles 1 and 3, no secondary hinge).

(e) Other solar paddle hinge-to-strut fasteners yielded only slightly (paddles 2 and 4, with secondary hinges).

This "fortunate misfortune" pointed out the point-of-failure of each appendage. Since over-spin was in the realm of possibility during launch, each of these areas was modified to have a greater margin of safety, as listed below:

1. Inertia boom hinge fasteners into shelf increased from 3 to 5. A change to stainless steel offers only little change, since only 1 1/2 D female thread length is available in the aluminum shelf.

2. Fasteners for all other appendage hinges to shelf applications were changed to stainless steel threaded through the strut and locked into position with a jam nut on the far side of the strut.

3. A doubled nylon cord was used to link each experiment boom to the escapement.

Figures 16, 17, and 18 show the test configurations at LRC.

Spacecraft—Vehicle Fit Test

This test cannot be overlooked, even though it did not involve the structure with strength, stiffness, or ability to resist fatigue considerations. The pre-prototype was completely outfitted with every component that could or would create an interference problem with the Delta heat shield. The complete payload outline—that is, spacecraft, separation system, Dutchman,

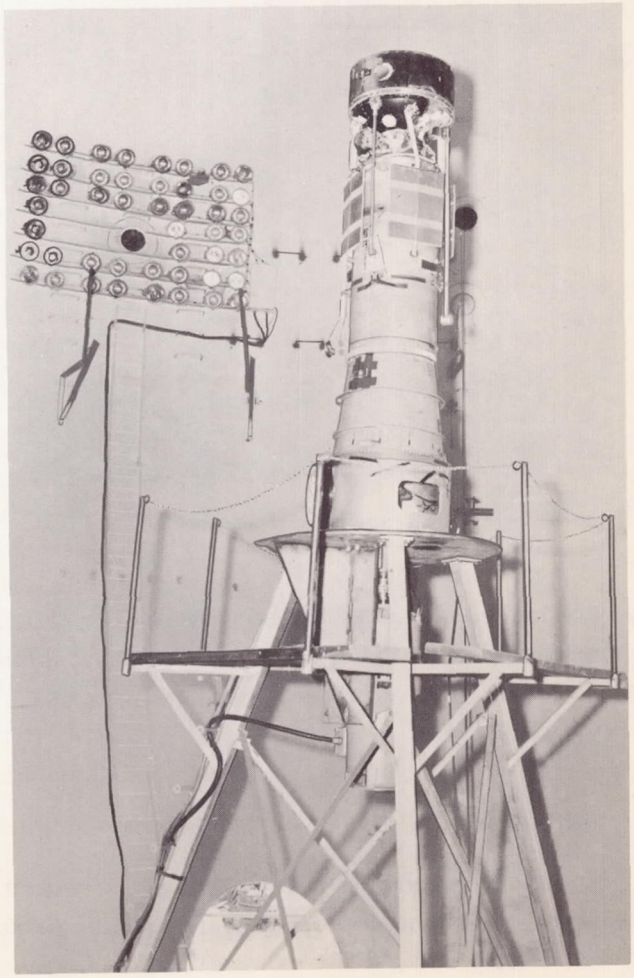

Figure 16—Pre-prototype setup for spin-up tests at LRC 60-ft vacuum facility.

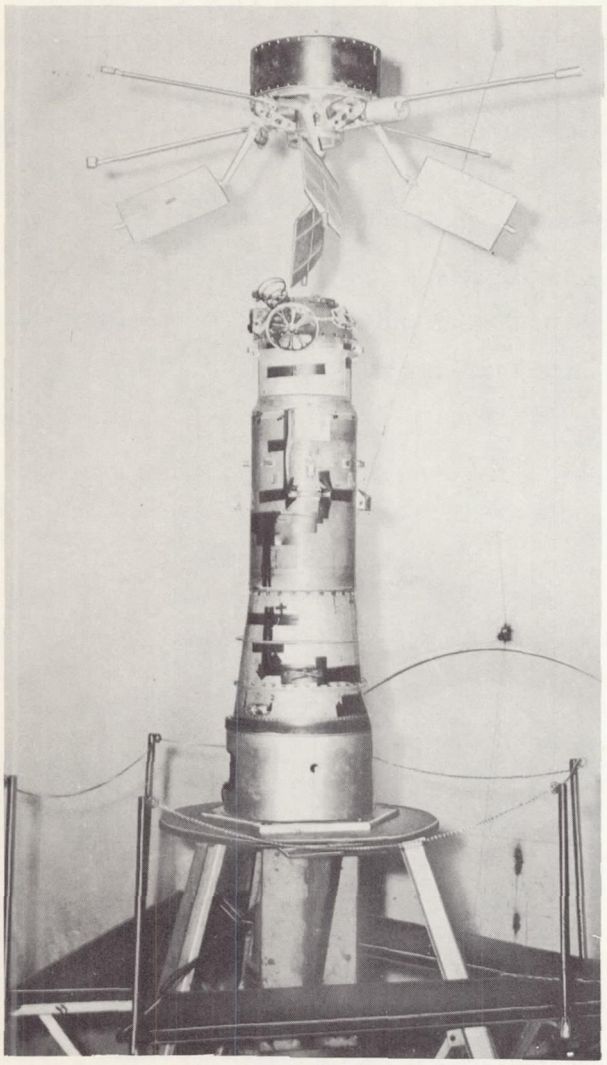

Figure 17—Pre-prototype after a separation test at LRC.

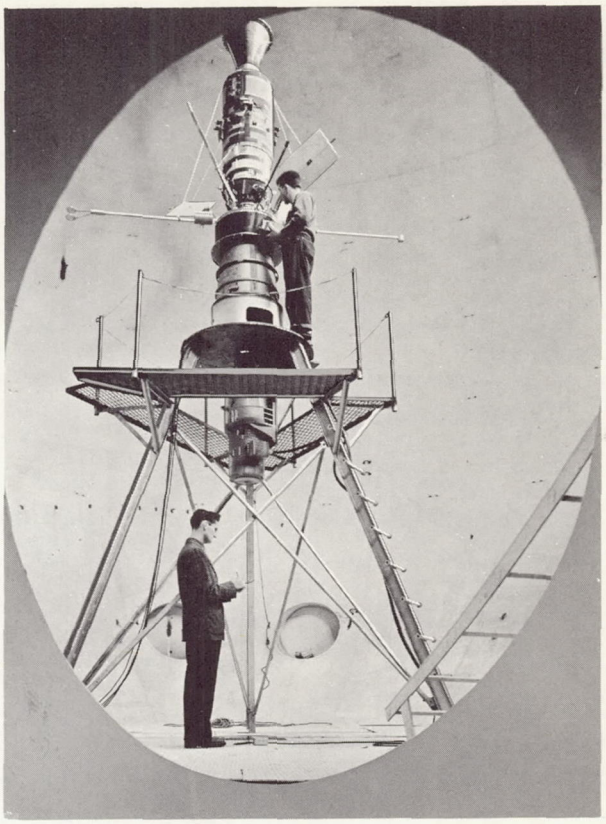

Figure 18—Pre-prototype after a de-spin test series at LRC.

release system, quadraloop antenna for the vibration experiment, interconnecting electrical cabling—was fitted together at Douglas (Santa Monica) on a dummy X-248 rocket motor. The heat shield was then fitted into position. No interference resulted. During this period the payload antenna ramps designed by GSFC and by Douglas (DAC) were tested for suitability. The DAC ramps were heavier than those of GSFC but, being larger, were deemed more satisfactory and after some modification were accepted for flight use. Figures 19, 20, and 21 show sample photo coverage of this fit test.

Erection Qualification Tests

The pre-prototype, not yet "retired," served to conduct a lengthy series of erection qualification tests for redesigned secondary hinge paddle arms 2 and 4 and for calibrating escapement devices in preparation for flight (Reference 6). The engineering test unit was prepared with the RF coating of copper, outfitted with a "final design" set of dummy appendages, and used as the vehicle by which all antennas were matched and the final antenna patterns determined.

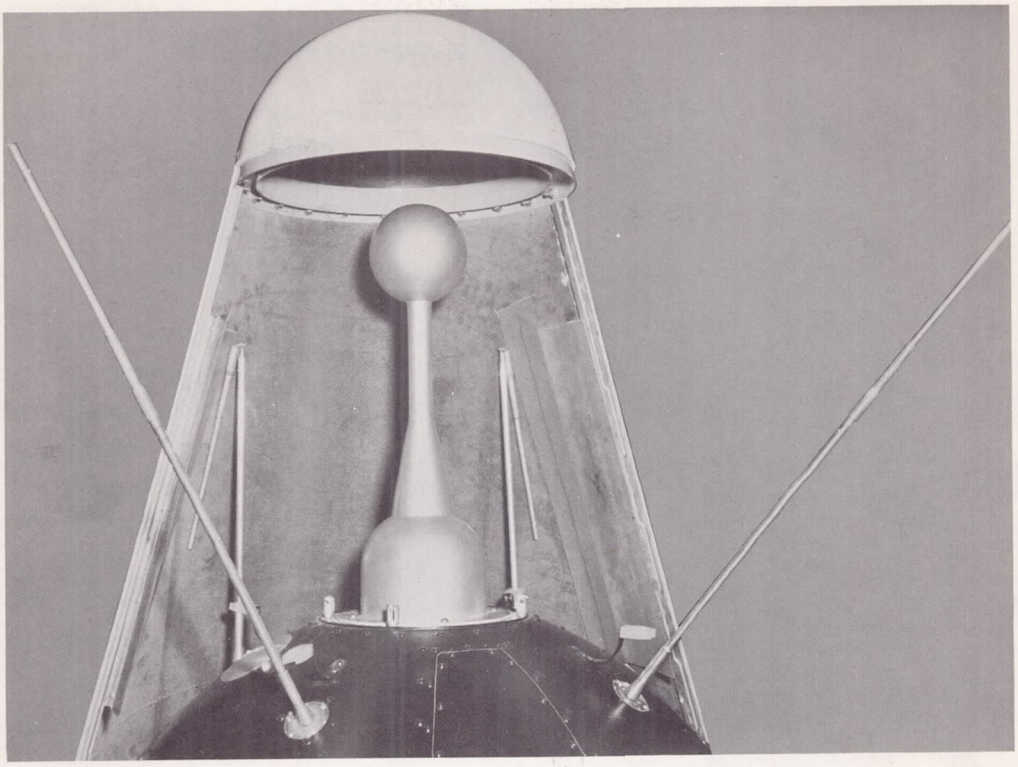

Figure 19—Antenna ramps in Delta heat shield.

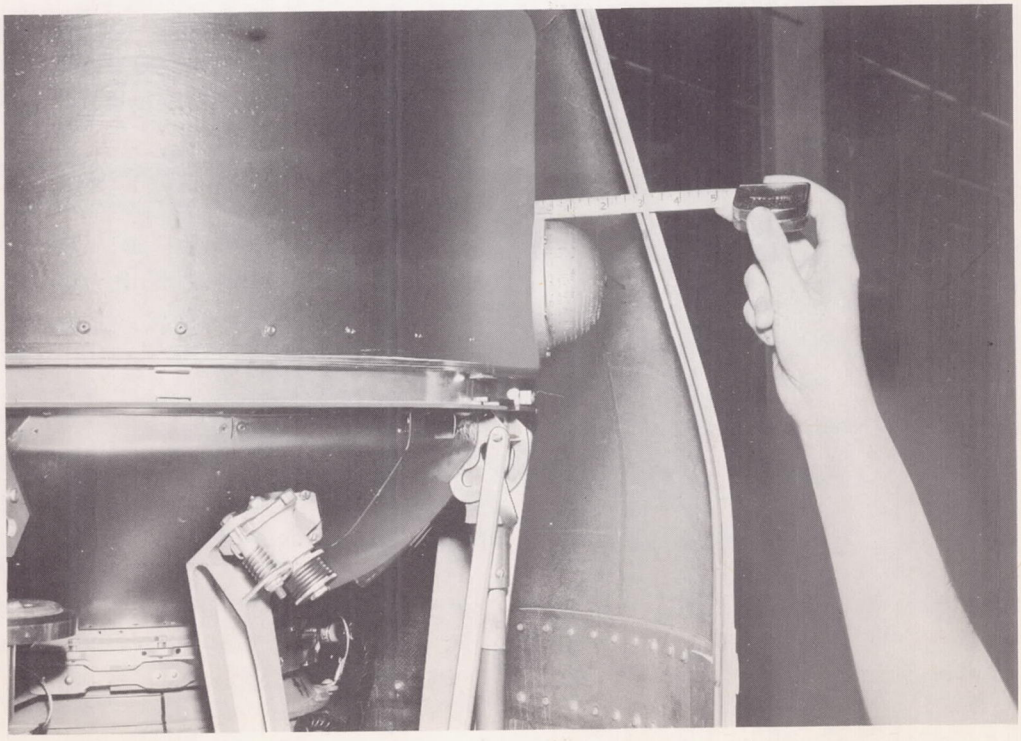

Figure 20—Aspect gage clearance in Delta heat shield.

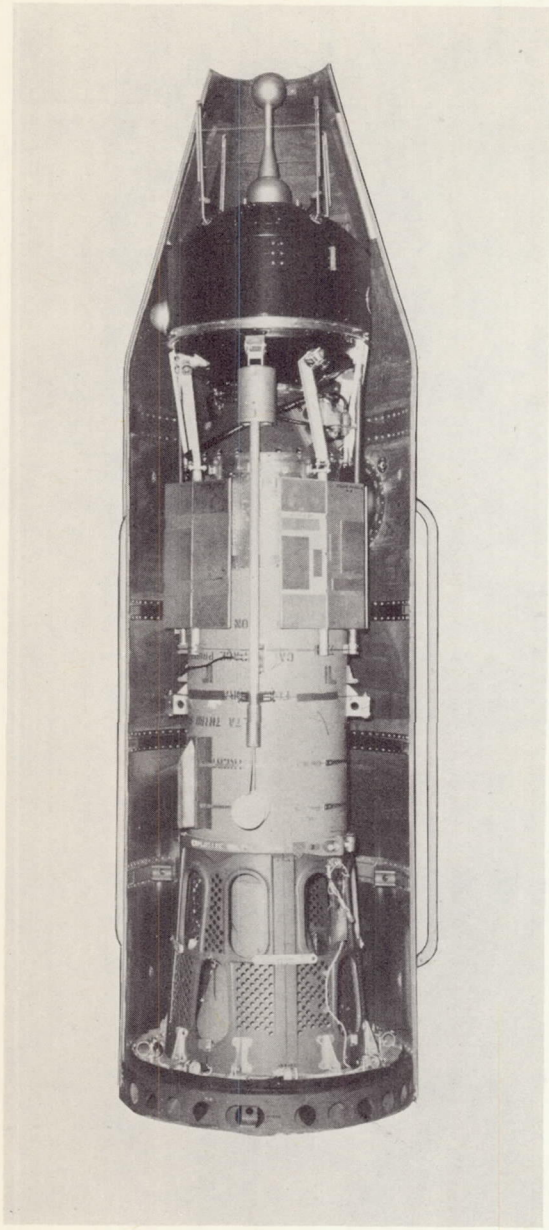

Figure 21—Ariel I-Delta vehicle fit test.

Prototype and Flight Model Tests

As a result of such extensive design testing, the Prototype and Flight Model Qualification Test series was nearly anticlimatic to the structure development. Even so, certain changes and test additions require that the tests and conditions be listed as follows:

1. As a result of "changing horses midstream"—that is, switching from Scout to the Thor-Delta three-stage vehicle—certain changes became necessary. The major change was the addition of a spacer, or Dutchman, which relocated the spacecraft 12 3/8 inches forward of its Scout position. The Delta third stage flies from a petal-leaf skirt, whereas the Scout fourth stage (same basic X-248) separates from its previous stage via a blastaway diaphram located at the aft interface of its skirt. The position change was required to allow the petal-leaf skirt to split without impacting on the experiment booms. The presence of the Dutchman in the dynamic assembly caused an increase in "g" input to the spacecraft because of its transmissibility (Q = 2) at the system resonance of 175 to 180 cps. The Chance Vought separation assembly also contributed to added inputs to the spacecraft; its transmissibility factor is 3.

2. The vibration levels were essentially the same as those of the ETU tests except that the vibration input was at the Dutchman, not directly to the spacecraft. Thus the above-mentioned transmissibility factors created a more severe test to the payload (see Appendix B). Two vibration test series were run on the prototype structure.

3. Steady-state acceleration tests were run on the prototype—the directions and levels the same as on the ETU. (See Table 1, page 15.)

4. The prototype spacecraft was subjected to a booster ignition shock test. No failure was experienced as a result of the test. Test conditions were three half-sine pulses of 30 g's in the thrust direction. Total time of the shock pulse was 10 to 15 milliseconds.

5. Temperature-humidity tests simulated possible ambient conditions that the payload might be required to withstand (should airconditioning malfunction, for example). Some spotting

Table 2

Revised Thermal-Vacuum Test Procedure for the Ariel I Prototype System.*

Payload Status	Conditioning Time (hr)	Payload Operating (hr)	Chamber Condition
1. Setup and complete checkout (ABC) with x-ray windows taped and 1-yr timers energized	24	---	Ambient
2. With spacecraft operating, pumpdown to 1×10^{-4} torr	1	1	Pressure pulldown
Hot Test:			
3. Stabilize system at +47°C	6	---	1×10^{-5} torr, +55°C
4. System operating (a) Batteries on 100 percent charge (b) ABC checkout every 12 hr (c) Continuous 2-hr checks NOTE: Battery charging rate: 24 hr at 1.0 amp 12 hr at 1.5 amp	36	36	↓
5. Battery charger off, system on internal power (battery capacity test)	18	18	↓
6. Battery efficiency check (a) 30-min undervoltage batteries on 100 percent charge at 1.0 amp (b) System operating on internal power to undervoltage lockout	3	---	↓
7. System on external power (a) Batteries on 100 percent charge (charging rate, 1.0 amp) (b) ABC checkout at start of 12-hr test (c) Continuous 2-hr checks	12	12	↓
8. ABC checkout at end of hot test, payload off, no charging of batteries	4	4	↓
Cold Test:			
9. Emissivity Test (a) Set chamber to -30°C. When temperature of wall reaches -20°C, reset chamber controller to -20°C (lower limit of sensors on the outer surface of the payload is -20°C)	10	---	1×10^{-5} torr, -20°C
10. Stabilize system at -10°C	8	---	1×10^{-5} torr, -10°C
11. System on internal power (a) No battery charging (b) ABC checkout every 12 hr (c) Continuous 2-hr checks	18	18	↓
12. Battery efficiency check (a) 30-min undervoltage batteries on 100 percent charge at 1.0 amp (b) System on internal power to undervoltage lockout	3	3	↓
13. Battery capacity test (a) System on external power (b) Batteries on 100 percent charge at 1.5 amp for 12 hr (c) Turn off external power, operate system to undervoltage	12	12	↓
14. End of cold test, system off	18	18	↓
30° Solar Aspect:			
15. Stabilize system with light ring no. 1 (+30°C on top of stack 2)	12	---	1×10^{-5} torr, -60°C
16. Spacecraft operating (a) ABC checkout every 12 hr (b) Continuous 2-hr checks (c) Turn heat lamps off for shadow effect (40 min)	12	24	↓
17. End of 30° solar aspect test, system off			↓
135° Solar Aspect:			
18. Stabilize system with light ring no. 2 (+10°C under stack 2)	12	---	1×10^{-5} torr, -60°C
19. Spacecraft operating (a) ABC checkout every 12 hr (b) Continuous 2-hr checks (c) Turn heat lamps off for shadow effect (40 min)	12	24	↓
20. End of -135° solar aspect test. Return chamber to ambient conditions. Payload operated.	12	---	Atmos, +25°C
21. ABC checkout and analysis, end of thermal-vacuum test.	6	6	Atmos., +25°C
Total conditioning time†: 3.5 days Total system operating time: 7.0 days Total test time†: 10.5 days			

*The prototype was subjected to several false starts and two complete test periods - Table 2 covers one test procedure.

†Includes setup time of 1 day.

of uncoated aluminum surfaces of the prototype by deposit of warm water vapor occurred; no other damage existed. The temperature-humidity conditions were as follows:

Storage Tests:

1. -30°C (-22°F) for 6 hours
2. Raise through ambient to +60°C (+140°F) for 6 hours

Operational Tests:

1. -10°C (50°F)
2. +50°C (122°F)

Humidity Exposure:

95% relative humidity at 30°C (86°F) for 24 hours

6. Thermal-vacuum testing created no detrimental effects on the prototype structure (see Table 2 for conditions).

7. The spacecraft was spun at 200 rpm for 1/2 hour and was dynamically balanced to the required specifications as listed in the Thor-Delta Restraints Document.*

8. The prototype structure was used in measurements of moments of inertia in the following conditions:

(a) I_{spin} - appendages open and closed,

(b) I_{xx} and I_{yy} - with appendages open and closed.

9. The flight units were subjected to vibration, temperature, and thermal vacuum evaluation (see Table 3); spin and balance procedures; and moment of inertia measurements. The input levels were basically the same as the flight levels experienced by the engineering test unit; exact values are listed in References 2 and 3; Appendix B also lists the vibration inputs.

Table 3

Thermal-Vacuum Test Flight Levels for Ariel I (Chamber Environment).

Sequence	Period (hr)	Environment	
		torr	°C
Evacuation	3	To 1×10^{-5}	--
Emissivity test	10	1×10^{-5}	-10°
Low temperature soak test	62	1×10^{-5}	-3°
Battery life test*	26	1×10^{-5}	-3°
Emissivity test	10	1×10^{-5}	+50°
High temperature test	62	1×10^{-5}	+40°
Battery life test*	26	1×10^{-5}	+40°

*Includes estimated time to drain power until payload enters "undervoltage" condition plus 18 hours of undervoltage.

*Delta Restraints Manual I-623-62-118, prepared by Douglas Aircraft Company, Inc. (Contact Delta Project Office, Spacecraft Systems and Project Division, Goddard Space Flight Center.)

FIELD OPERATIONS

The satellite was shipped by air to the Atlantic Missile Range, Cape Canaveral, Florida, in dust-free shipping containers. Once there, it was electrically assembled for a pre-checkout and then was mechanically assembled at the antenna field for T/M antenna pattern determination and electron density experiment final calibration. This required manhandling of the package onto the 10-foot-high platform and back down again. After final calibration, the unit was mated with the X-248 last stage engine at the spin balance facility. At this point the electron density experiment was damaged, and boom replacement required a repeat of the above field calibration.

During final payload–X-248 mating, the escapement pallet was found to have fatigued; a complete escapement replacement was installed. All flight appendages were restrained with the flight release hardware, and the total assembly was dynamically balanced at a 190 to 200 rpm spin rate. This complete assembly was then transported in a dust-free transportainer to the gantry to be mated with the Delta second stage. One day prior to launch, the water-emulsion latex-base strippable coating was removed, and the outer surfaces of the satellite were cleaned of smudges, fingerprints, etc.

During this first countdown a malfunction was found in the vehicle, and the launch was "scrubbed" for 15 days. To repair the vehicle, the third stage - payload assembly was removed from the vehicle and stored in the spin facility. The satellite was not recoated but was contained in the Douglas transportainer.

Final mating took place on April 21, 1962, with no further delays; and Ariel I was on standby ready for launch.

Flight

Only one more trial was required of the Ariel I structure: to successfully carry into orbit the experiments and electronic components that combine to form the satellite. That the structure did properly serve its function is fact; however, the rigors experienced during the launch should also be discussed.

The trajectory of all three stages was as expected - in fact, very nearly nominal; therefore, the powered phase of the launch produced the accelerations and vibrations as predicted and tested for. However, starting 100 seconds after ignition of the third-stage X-248 rocket motor, the spacecraft experienced four unnatural, premature, rapid de-spin sequences: The spacecraft rotational velocity changed from 158 to 122 rpm; then to 100 rpm; then to 90 rpm, and finally to 78 rpm in periods of less than 0.5 second each. A careful correlation of moment of inertia changes versus spin rate changes indicated premature erection of appendages in the following order:

(1) Two adjacent solar paddles and one inertia boom

(2) An experiment boom

(3) A second experiment boom

(4) The final two solar paddles and inertia boom

The spacecraft again saw rotational velocity changes: Three de-spin sequences occurred at the prescribed time schedules. The first of these was undoubtedly due to yo-yo release, and the other two de-spins may have been due to pin puller release action (see Appendix C). The point to be emphasized is that, if the premature erection sequences listed above did occur, the structure received far more serious stresses than normal erection would impart. Had not the design test series been as stringent as it was—and action taken to increase margins of safety where deemed necessary—Ariel I surely would have lost at least part of her appen[illegible]ing the premature de-spins.

CONCLUSIONS AND RECOMMENDATIONS

The end result of nearly two years of effort in design, development integration, and testing of the Ariel I structure was the successful launching and orbiting on April 26, 1962. The structure certainly became more and more complex as the total satellite was developed. The state-of-the-art in RF and thermal coating of fiber glass advanced because of Ariel I. Fiber glass structures and mechanisms can efficiently be utilized in space applications. Although the stretch yo-yo did not get the chance to fully prove itself in flight, its use can be condoned as a result of the design test program developed for it.

The following items should be investigated in the light of further usefulness in the design and development of future spacecraft structures and mechanisms:

1. The structural use of fiber glass thin-wall cylinders and tubes made of epon-bonded cloth of fiber glass versus the more costly filament-wound fiber glass.

2. The practicability of all-bonded structural joints, especially in fiber glass to metal, or of dissimilar metal interfaces.

3. The use of fine filaments of RF shield metal (copper, aluminum, etc.) manufactured integrally with the fibrous glass structure.

4. Higher temperature bonding agents should be sought and utilized for non-metal structures.

The knowledge gained from the design, development, and testing of the Ariel I structure will in no small measure contribute to the continued success of GSFC-built spacecraft.

ACKNOWLEDGMENTS

The author wishes to thank the staff of the Langley Research Center's 60-Foot Vacuum Test Sphere Facility for their contribution to the success of the spin-up, de-spin test series that proved the worthiness of Ariel's appendages. The personnel of the GSFC Thermal Systems Branch deserve much credit for their successful efforts in developing a unique surface coating that provided the proper thermal, electrical, and RF properties for the fiber glass structure of the satellite.

REFERENCES

1. Eng, T. L., "Energy Absorber for the Ariel I Instrument Booms," NASA Technical Note D-1857, 1963 (In press).

2. Cornille, H. J., Jr., "A Method of Accurately Reducing the Spin Rate of a Rotating Spacecraft," NASA Technical Note D-1420, October 1962.

3. Fedor, J. V., "Analysis of the Stretch Yo-Yo for De-Spin of Satellites," NASA Technical Note D-1676, April 1963.

4. Conn, J. H., and Sutton, J. F., "Report of Environmental Vibration Test - - Structural Model No. 1, International Ionosphere Satellite, S-51," Goddard Space Flight Center 321.2(JC)S-51-11, June 1961.

5. Forsythe, R. W., "A Method for Simulating Zero Gravity Erection of Satellite Appendages," NASA Technical Note D-1852, 1963 (In press).

6. Forsythe, R. W., "Analysis of Dissimilar Satellite Appendages During Erection," NASA Technical Note D-1688, 1963 (In press).

Appendix A

Physical Measurements of Ariel I

Included in this appendix are the weights, centers of gravity, and moments of inertia of Ariel I, flight unit 1.

Weight (lb):

Payload Structure (see weight table)	50.56
Yo-yo springs and end masses	2.00
University College London experiments	21.53
Imperial College experiments	5.70
University of Birmingham experiments	8.29
GSFC non-structure components (electronics, power supply, harness, tape recorder, etc.)	47.72
Total Spacecraft Weight	135.80

Center of gravity, forward of separation plane (in.):

All components folded	5.96
All components extended	8.13

Moments of inertia* (slug-ft^2):

All components folded

I_{xx}	5.25
I_{yy}	4.75
I_{zz}	1.99

*All measurements are referenced to the three principal axes in Figure A1; zz is the spin axis.

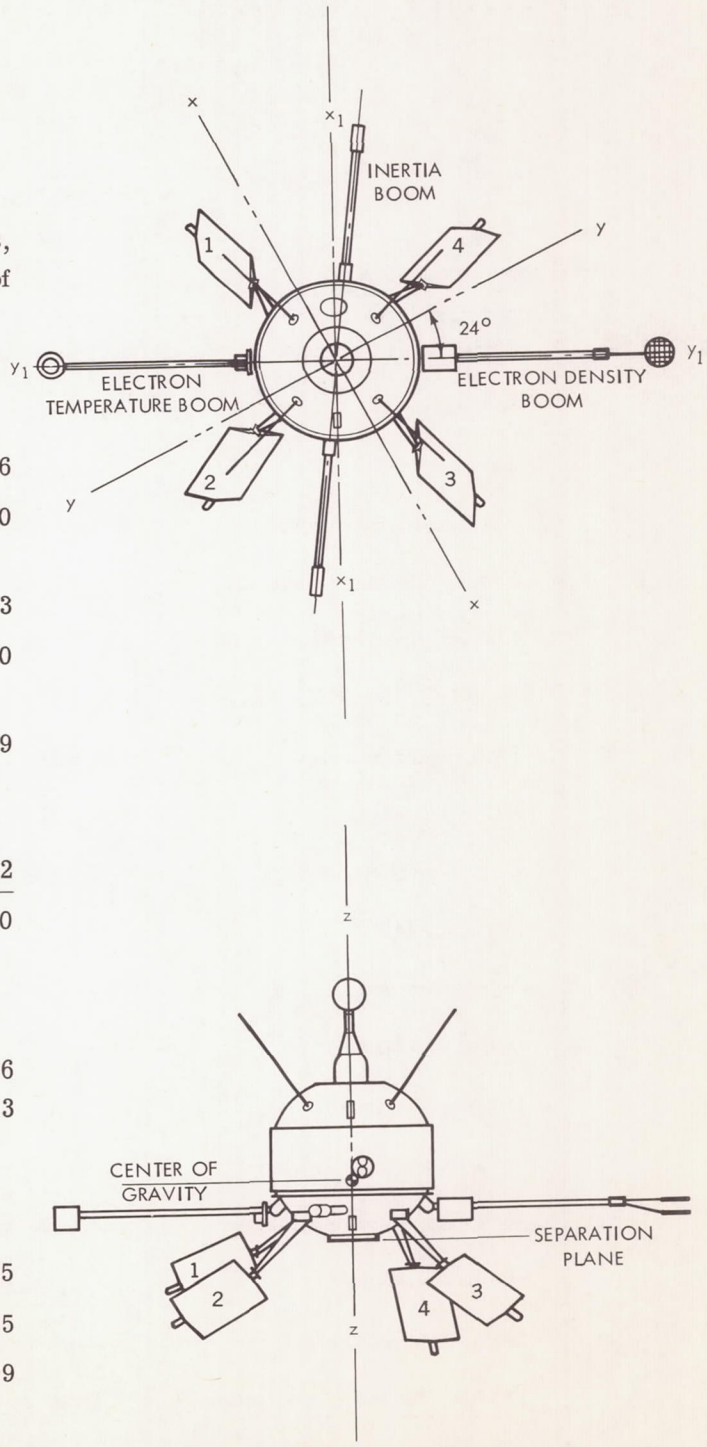

Figure A1—Location of spacecraft's principal axes.

All components extended (orbit condition)

I_{xx} 5.13

I_{yy} 4.03

I_{zz} 5.48

I_{zz}/I_{xx} 1.07

Table A1

Structure and Mechanism Weights.

Item	Remarks	Weight (lb)
Upper dome	Includes thermal and RF coating	6.53
Mid-skin	Includes thermal and RF coating	6.80
Lower dome	Includes thermal coating	1.52
Shelf and base assembly	Shelf, struts, base, fasteners	12.63
Paddle arms and hinges (4)	Includes interface fasteners	4.36
Inertia booms and hinges (2)		3.85
Experiment boom hinges (2)		0.87
Escapement assembly	Includes nylon guides	1.54
De-spin housing	Includes guillotines (2)	1.76
De-spin weights and springs	Excluded from orbit weight	2.00
Antennas (4)		0.80
Separation adapter ring	Includes interface fasteners	0.51
Battery containers	Includes battery spacers	3.05
Dynamic balance		1.93
Turn-on plug and housing		0.14
Base closure plate assembly	Includes interface fasteners	1.07
Harness bracketry	Includes clamps, fasteners	1.34
Component bracketry	For non-structural components	0.91
Internal thermal equilization	Surface coatings and heat sinks	0.97
	Total Structure and Mechanisms:	52.58

Appendix B

Ariel I Vibration Specifications

Vibration Test Schedule

Included herein are vibration test schedules for (I) prototype levels and (II) flight acceptance levels.

I. Prototype Levels:

Table B1

Frequency Sweep Schedule

Vibration Axis	Frequency Range (cps)	Test Duration (min)	Acceleration, 0-to-peak (g)
Thrust (z-z)	5-50	1.66	*2.3
	50-500	1.66	10.7
	500-2000	1.00	†21
	2000-3000	0.30	54
	3000-5000	0.36	21
		Total: 4.98	
Lateral (x-x) and Lateral (y-y)	5-50	1.66	*0.9
	50-500	1.66	2.1
	500-2000	1.00	4.2
	2000-5000	0.66	†17
		Total: 4.98	

*Within maximum amplitude limit of vibration generator.
†Within maximum frequency limit of vibration generator.

Random Motion Vibration - Gaussian random vibration shall be applied with g-peaks, clipped at three times the root-mean-square acceleration, according to the schedule given herein. With spacecraft installed, the control accelerometer response shall be equalized such that the specified PSD values are within ±3 db everywhere in the frequency band. The filter roll-off characteristic above 2000 cps shall be at a rate of 40 db/octave or greater.

Table B2

Random Vibration Schedule.

Vibration Axis	Frequency Range (cps)	Test Duration (min)	PSD Level (g^2/cps)	Approximate rms Acceleration (g)
Thrust (z-z)	20-2000	4	0.07	*11.5
Lateral (x-x) and Lateral (y-y)	20-2000	4 (*each axis*)	0.07	*11.5
Grand total: 12 minutes				

*Within amplitude limit of vibration generator.

Combustion Resonance - This test simulates a measured combustion oscillation condition observed in the X-248 solid-propellant rocket motor. The range of the sinusoidal vibration test is from 550 to 650 cps. The test is conducted by traversing this 100-cps-wide band slowly such that 1/2 minute is consumed in moving from 550 to 650 cps. Rate of change of frequency with time shall be proportional to frequency.

Apparent weight of the spacecraft is assumed to be 7 pounds. Using this assumption, the control acceleration should be ±86g (0 to peak) for the thrust axis and ±14.5g (0 to peak) for the lateral axes.

II. Flight Acceptance Levels:

Table B3

Frequency Sweep Schedule.

Vibration Axis	Frequency Range (cps)	Test Duration (min)	Acceleration, 0-to-peak (g)
Thrust (z-z)	5-50 50-500 500-2000 2000-3000 3000-5000	0.83 0.83 0.50 0.15 0.18 Total: 2.49	*1.5 7.1 14 36 †14
Lateral (x-x) and Lateral (y-y)	5-50 50-500 500-2000 2000-5000	0.83 0.83 0.50 0.33 Total: 2.49 (each axis)	*0.6 1.4 2.8 †11.3
Grand total: 7.5 minutes			

*Within maximum amplitude limit of vibration generator.
†Within maximum frequency limit of vibration generator.

Random Motion Vibration - Instructions are the same as for prototype levels: however, the random vibration schedule is as follows:

Table B4

Random Vibration Schedule.

Vibration Axis	Frequency Range (cps)	Test Duration (min)	PSD Level (g^2/cps)	Approximate rms Acceleration (g)
Thrust (z-z)	20-2000	2	0.03	*7.7
Lateral (x-x) and Lateral (y-y)	20-2000	2 (each axis)	0.03	*7.7
Grand total: 6 minutes				

*Within amplitude limit of vibration generator.

Combustion Resonance - Instructions are the same as for prototype test except levels shall be ±57g (0 to peak) in the thrust axis and ±9.4g (0 to peak) in the lateral axes.

Appendix C

Aspect Sensor Observations on Ariel I During Launch

by
Dr. A. P. Willmore
University College London

Introduction

This is an account of observations made on the behavior of the Ariel I using solar aspect indicators. The observations cover the period from spin-up of the third stage to about 6 minutes after separation. Measurements were made at various times of spin rate, solar aspect angle, and nutation or coning angle.

The aspect sensor used consisted of a combination of curved slits and solar cells, from the output of which the above quantities could be deduced. One such sensor was mounted on the payload Dutchman and another on the spacecraft. The output from the Dutchman sensor was directly telemetered using an information bandwidth of 1000 cps on a 240-Mc carrier. The output from the payload sensor was subjected to a considerable amount of in-board processing and then transmitted by three channels of the spacecraft 136-Mc telemetry.

240-Mc telemetry of good quality was received at Antigua. It was also received by O. R. V. Whiskey, located at the mouth of the Amazon; but the reception was marred by many fades. 136-Mc telemetry of fair quality was received by H.M.S. Jaguar, located at Tristan da Cunha. Unfortunately this record did not contain any time signals. Accordingly the time scale for these observations was obtained by identifying the de-spin due to yo-yo deployment, and assuming that this occurred as planned 15 minutes after third-stage ignition.

Results

Times of Spin-Up and Third-Stage Ignition

Time* of spin-up was $18^h10^m55^s.04$

Time of pressure switch closure was $18^h11^m14^s.00$

*All Times are UT.

Aspect Angle

The measurements are plotted in Figure C1. The aspect angle defined here is the angle between the satellite-sun line and the forward direction of the spin axis in the launch configuration. It will be seen that the initial value is close to that calculated for a nominal orbit, which is 84 degrees. The angle slowly increases after 18^h25^m, the time of the first observation from H.M.S. Jaguar, reaching a steady value at about 18^h33^m of 43 degrees. This was also the value obtained at the end of the first orbit.

Since the precession between $18^h10^m56^s$ and $18^h18^m20^s$ is observed to be small, 2 degrees or less, the change in aspect angle between 18^h25^m and $18^h28^m30^s$ (which is the expected time of separation) must be due to nutation. Since the sun line is nearly perpendicular to the spin axis, nutation will be observed as a change in aspect, the complement of the aspect angle being $2/\pi$ of the nutation angle. It should be noted that time taken for the circuitry to process the date is comparable with the time scale of the phenomena, so that the measured angles are lower limits.

Nutation Angle

The semi-angle of the nutation cone is plotted as a function of time in Figure C2. Some of the points as indicated on the graph were obtained from the Dutchman aspect system directly, while the others were deduced as explained in the last paragraph from the aspect angle. The point marked at

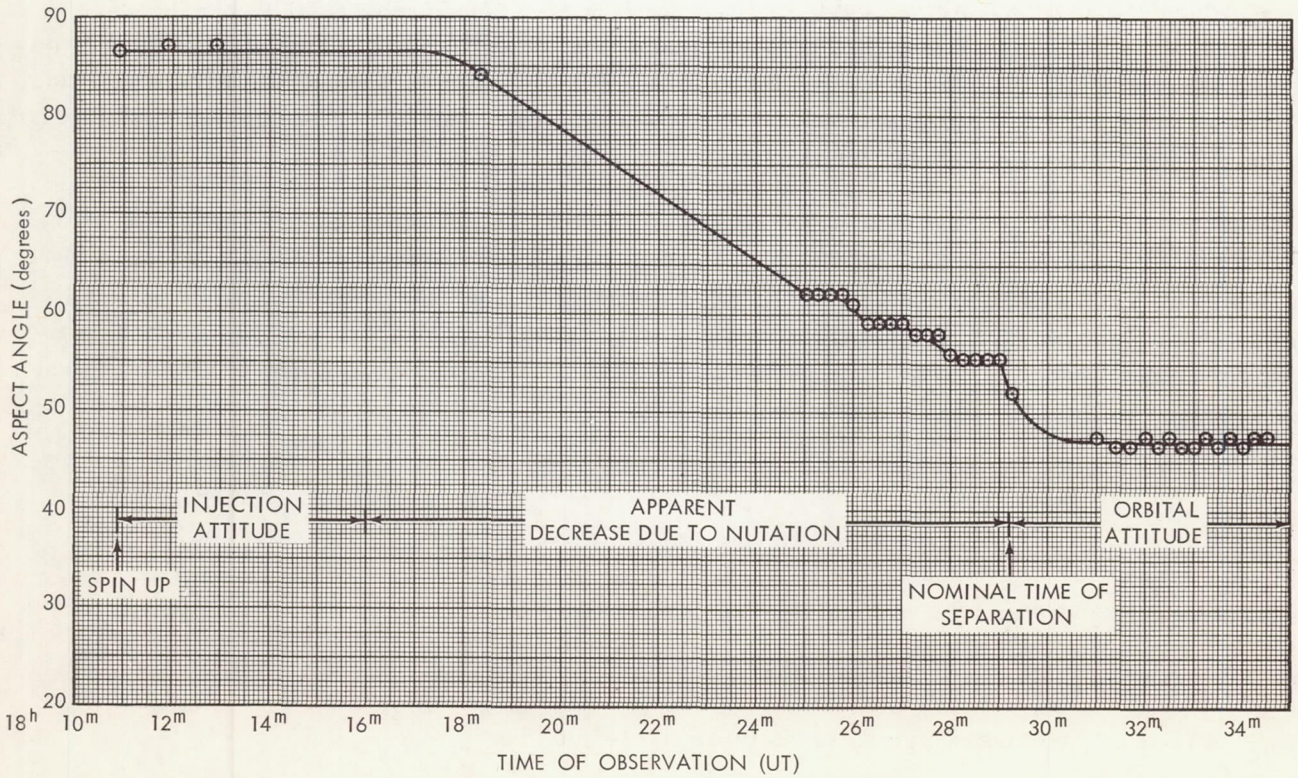

Figure C1—Aspect angle measurements.

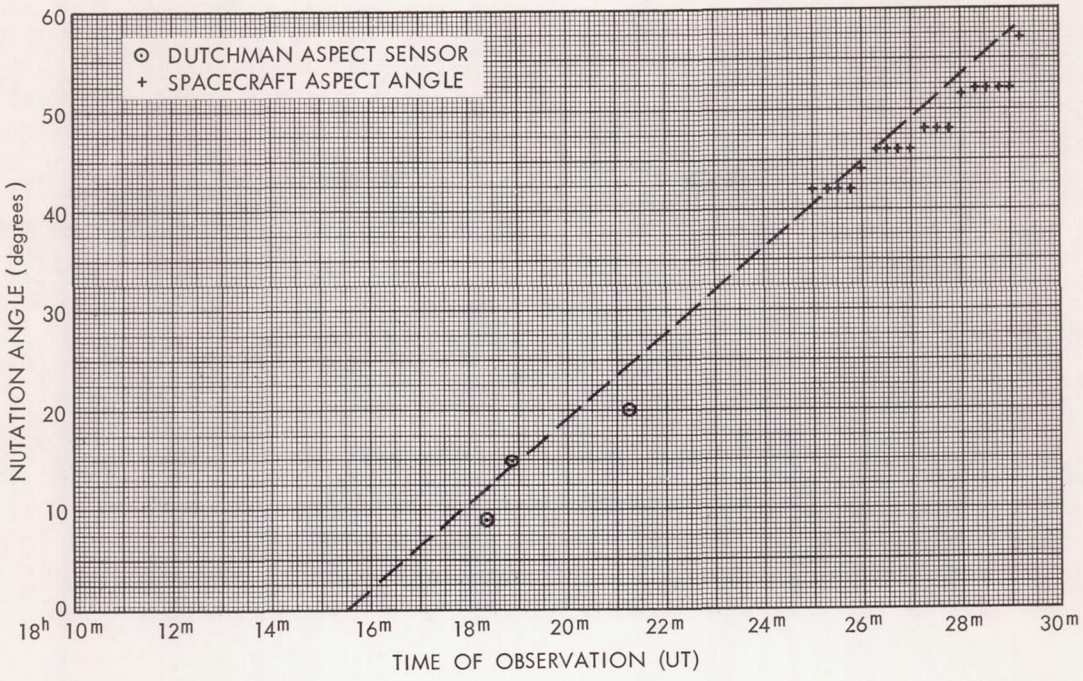

Figure C2—Nutation cone semi-angle as a function of time.

$18^h21^m9^s$ is certainly only a lower limit to the nutation angle. At this time the telemetry was subject to regular fades at the nutation rate, so that data over the same part of the cycle were always lost.

Another method of deducing the nutation from an apparent oscillation in the spin rate was so used. This gave erratic and sometimes absurd results. It is believed that this was due to a sensitivity of the circuitry employed to nutation at the observed period of about 10 seconds. The results were therefore rejected as unreliable.

It will be seen that the measurements are roughly consistent with a constant increase of nutation angle of 4 degrees per minute from 18^h14^m to 18^h29^m, reaching a value of 58 degrees at the latter time.

Spin Rate

The measurements are shown in Figure C3; they can be separated into five phases. From the completion of spin-up at $18^h10^m56^s$, the spin rate increases to the end of third-stage burning. It then remains constant until $18^h12^m53^s.4$, after which it decreases in four well-defined steps to 78 rpm at $18^h14^m15^s$. This is the second phase. The third lasts until $18^h25^m30^s$. From $18^h18^m20^s$ to $18^h21^m9^s$, the spin rate diminishes continuously, not in steps, and this is presumably true throughout the third phase. From $18^h25^m30^s$ to $18^h28^m30^s$, the rate once again diminishes in steps, and finally from $18^h28^m31^s$ it reaches the value of 38.2 rpm, which was measured also at the end of the first orbit.

The anticipated spin rate variation with time is also marked on the graph. Apart from the agreement of the initial and final values, there is very little correspondence.

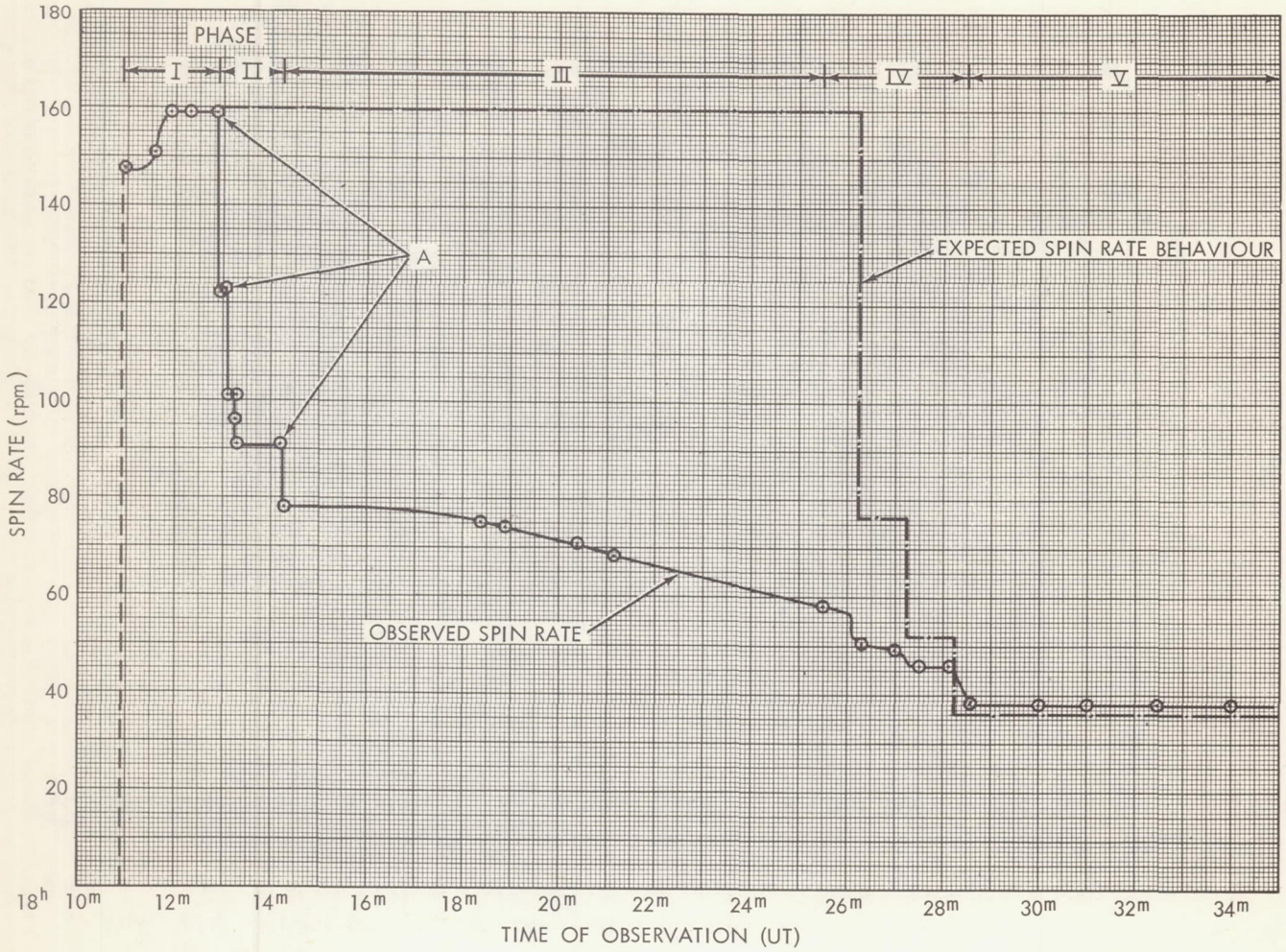

Figure C3—Spin rate measurements.

Figure C4 shows the calculated relation between spin rate and nutation angle (calculated by R. Forsythe). It is immediately clear from Figure C2 that the spin reduction in phase II cannot arise from nutation. It must therefore correspond either to a reduction of angular momentum or an increase in moment of inertia such as would be caused by the premature erection of the booms and paddles in four stages. The later interpretation is supported by two observations.

The Dutchman carried also three orthogonally mounted accelerometers as vibration pickups. Three of the de-spin events—marked "A" in Figure C3—are accompanied by short duration shocks, such as might be caused by the booms snapping into place. The spin reduction is in these cases complete in about 0.5 second, and it is clear from the records that the reduction is complete by the time that the shock occurs. This is consistent with boom erection rather than the exertion of external impulses (as from motor "chuffing"), where the de-spin accompanies the impulse. For the fourth de-spin, where there is no shock, the duration of de-spin is slightly greater. The moment of inertia change corresponds with the erection of an experiment boom, so that this boom might have been successfully restrained by the escapement fitted for the purpose.

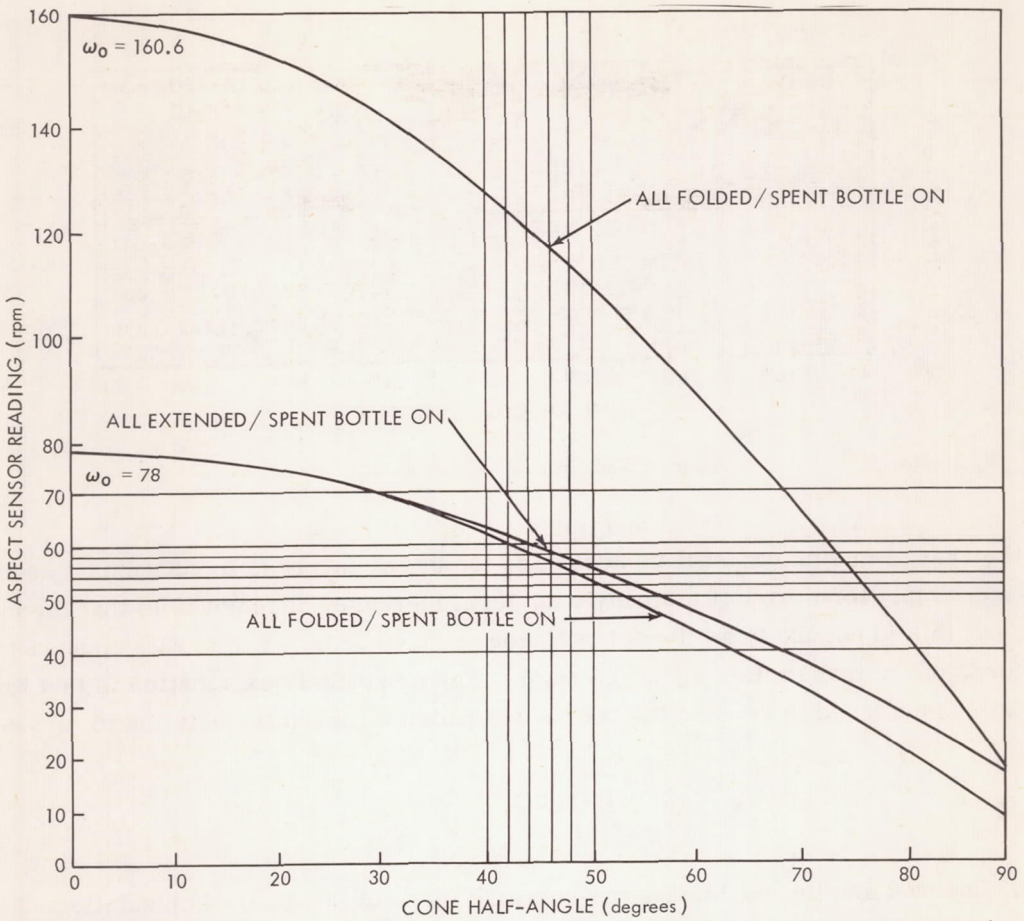

Figure C4—Relation between spin rate and nutation angle (assuming coning due to unrigid body and adverse I ratio only).

Moreover, some 136-Mc telemetry was also received at Antigua. This shows a sudden and very marked change in the null of the electron density experiment at about this time, confirming that the boom erected here.

The reduction in spin rate through phase III can be explained by the increasing nutation. The results of Figure C2 have been smoothed by passing a straight line through them. From this, the spin rate variation with time has been calculated from Figure C4. The result is plotted in Figure C5 as the solid line. The measured values of spin rate are also marked. It can be seen that throughout this phase there is a good agreement.

The values from phase IV fall close to an approximately parallel line, corresponding to a spin rate some 10 percent lower throughout. Presumably this is due to the yo-yo de-spin at $18^h25^m30^s$. Thus it seems that the entire de-spin in phases III and IV is accountable in terms of the increasing nutation over this period, together with the yo-yo de-spin.

There is, however, a slight difficulty in this explanation. A close examination of Figures C2 and C3 reveals that the changes of spin rate and nutation angle during phase IV do not appear to occur smoothly but in steps, at 1-minute intervals.

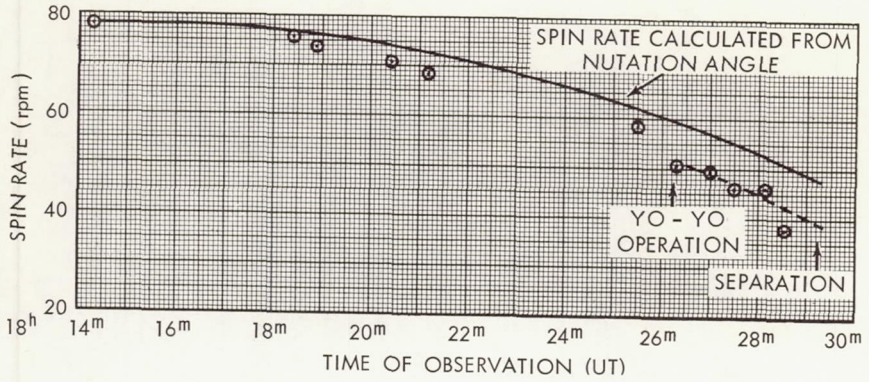

Figure C5—Spin rate variation with time.

While the change in spin can still be accounted for by the increase in nutation, it seems that the latter does not simply form part of a steady long-term increase. It is possible that the effect is experimental, but this is not likely as the discontinuous behaviour of the spin rate appears corroborated by AGC records of the transmitter signal strength. The most likely explanation is that the operation of the pin-pullers designed to release the booms and paddles caused the nutation to increase.

Conclusions

Spin-up occurred as planned, leaving the spin axis close to the desired orientation. The erection of the booms and paddles occurred prematurely about 1-2 minutes after injection. An increasing nutation then occurred because of the long coast time and the unfavourable moment of inertia ratio, reaching a semi-angle of cone of 58 degrees by separation. Separation occurred satisfactorily. It is interesting to note that the close agreement between the expected and actual values of the final spin rate is entirely fortuitous.

Acknowledgments

Many people have contributed in important ways to these observations and their interpretation. It is a pleasure to acknowledge this assistance.